

Consumption of dietary fat causes loss of olfactory sensory neurons and associated circuitry that is not mitigated by voluntary exercise in mice

Brandon M. Chelette^{1,2} , Ashley M. Loeven¹ , Destinee N. Gatlin^{1,2} , Daniel R. Landi Conde^{1,2} , Carley M. Huffstetler¹ , Meizhu Qi^{1,2}  and Debra Ann Fadool^{1,2,3} 

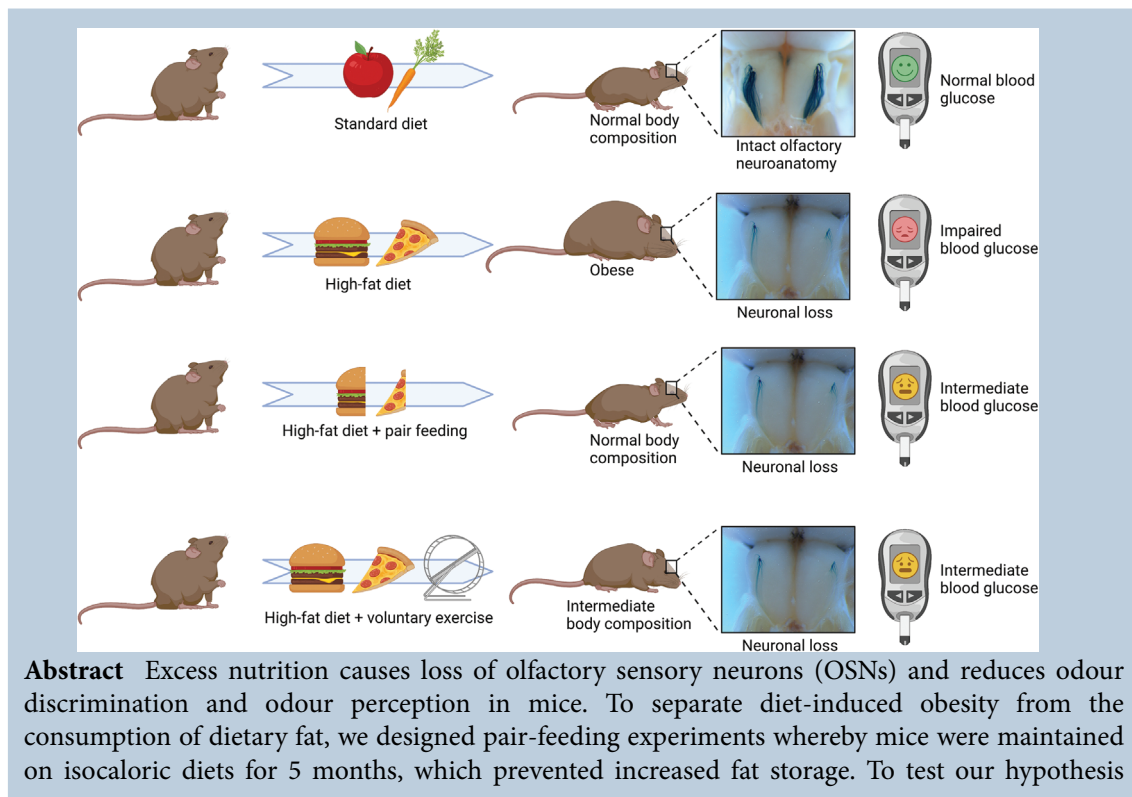
¹Department of Biological Science, Florida State University, Tallahassee, FL, USA

²Programs in Neuroscience, Florida State University, Tallahassee, FL, USA

³Molecular Biophysics, Florida State University, Tallahassee, FL, USA

Edited by: Ian Forsythe & Nathan Schoppa

The peer review history is available in the Supporting Information section of this article (<https://doi.org/10.1113/JP282112#support-information-section>).



Brandon M. Chelette previously completed his BSc in Biological Science at The Florida State University (FSU) as well as a PhD in Neuroscience from the same institution. His dissertation work focused on the effects of diet and exercise on the olfactory system, during which time he was a participant in the Chemosensory Training Program at FSU and lead scientific outreach in the community. He is currently a postdoctoral fellow in the Neuroimmunology Research Group at MD Anderson Cancer Center where he studies the impact of cancer and cancer treatments on fatigue and metabolism.



that adiposity was not a prerequisite for loss of OSNs and bulbar projections, we used male and female mice with an odorant receptor-linked genetic reporter (*M72tauLacZ*; *Olfr160*) to visualize neural circuitry changes resulting from elevated fat in the diet. Simultaneously we monitored glucose clearance (diagnostic for prediabetes), body fat deposition, ingestive behaviours, select inflammatory markers and energy metabolism. Axonal projections to defined olfactory glomeruli were visualized in whole-mount brains, and the number of OSNs was manually counted across whole olfactory epithelia. After being pair fed a moderately high-fat (MHF) diet, mice of both sexes had body weight, adipose deposits, energy expenditure, respiratory exchange ratios and locomotor activity that were unchanged from control-fed mice. Despite this, they were still found to lose OSNs and associated bulbar projections. Even with unchanged adipocyte storage, pair-fed animals had an elevation in TNF cytokines and an intermediate ability for glucose clearance. Albeit improving health metrics, access to voluntary running while consuming an *ad libitum* fatty diet still precipitated a loss of OSNs and associated axonal projections for male mice. Our results support that long-term macronutrient imbalance can drive anatomical loss in the olfactory system regardless of total energy expenditure.

(Received 2 July 2021; accepted after revision 5 November 2021; first published online 22 November 2021)

Corresponding author D. A. Fadool: Department of Biological Science, The Florida State University, 319 Stadium Drive, Suite 3008, King Life Sciences Building, Tallahassee, FL 32306, USA. Email: dfadool@fsu.edu

Abstract figure legend Patterns of long-term dietary consumption and exercise shape neuronal abundance and communication in the olfactory system. Design made in BioRender.

Key points

- Obesity can disrupt the structure and function of organ systems, including the olfactory system that is important for food selection and satiety.
- We designed dietary treatments in mice such that mice received fat, but the total calories provided were the same as in control diets so that they would not gain weight or increase adipose tissue.
- Mice that were not obese but consumed isocaloric fatty diets still lost olfactory neuronal circuits, had fewer numbers of olfactory neurons, had an elevation in inflammatory signals and had an intermediate ability to clear glucose (prediabetes).
- Mice were allowed access to running wheels while consuming fatty diets, yet still lost olfactory structures.
- We conclude that a long-term imbalance in nutrition that favours fat in the diet disrupts the olfactory system of mice in the absence of obesity.

Introduction

Chemosensory ability is dependent upon nutritional health and metabolic state for both humans and rodents, demonstrating that energy homeostasis is a driver of food detection and satiation (Lacroix *et al.* 2015; Kolling & Fadool, 2020). In both taste and olfactory systems, diet-induced obesity (DIO) or excess nutrition causes the loss of olfactory sensory neurons (OSNs) and taste buds, ultimately causing a reduction in chemosensory ability (Tucker *et al.* 2012b; Thiebaud *et al.* 2014; Lacroix *et al.* 2015; Kovach *et al.* 2016; Fardone *et al.* 2018; Kaufman *et al.* 2018). The impact of olfactory deficits in obese mice has been well studied (Palouzier-Paulignan *et al.* 2012). Obese mice have a reduced density of axonal projections to the olfactory bulb, a reduction in

G_{olf} and odorant receptor proteins and poorer odour discrimination using conditioned odour-aversion tasks, habituation/dishabituation trials, or go-no-go operant conditioning paradigms (Fadool *et al.* 2011; Tucker *et al.* 2012b; Aimé *et al.* 2014; Thiebaud *et al.* 2014; Lacroix *et al.* 2015; Fardone *et al.* 2018). Electrically, obese mice have a reduction in the receptor potential (Thiebaud *et al.* 2014; Lacroix *et al.* 2015) collectively generated from the population of OSNs, and acquired from the surface of the olfactory epithelium using a recording called an electroolfactogram (EOG; Scott & Scott-Johnson, 2002). Moreover, output neurons called mitral cells, which relay information to higher cortical regions from the olfactory bulb, have changed activity in obese rodents. In rodents with obesity, mitral cells have altered sensitivity to neuro-hormones such as insulin and are differentially modulated

by energy-important molecules (Fadool *et al.* 2011; Aimé *et al.* 2014). Low-grade, chronic inflammation brought on by DIO (Hotamisligil, 2006) has inhibited the renewal of taste buds (Kaufman *et al.* 2018); however, the mechanism of loss of OSNs in the olfactory system attributed to obesity remains less understood.

Two different transgenic mouse models have suggested that DIO may not be the direct or sole cause of loss of OSNs in the olfactory system. Mice with a loss of melanocortin-4 receptor (MC4R^{-/-}) in the hypothalamus present with late-onset diabetes and associated weight gain, have hyperleptinaemia and are hyperphagic (Tucker *et al.* 2008). MC4R is a G-protein-coupled receptor that when activated reduces food intake and increases energy expenditure (EE) through leptin signalling. Despite their genetically predisposed obesity, MC4R^{-/-} mice are not anosmic nor do they exhibit structural changes in OSN abundance or associated axonal projections (Tucker *et al.* 2008, 2012a; Thiebaud *et al.* 2014). Mice with a loss of voltage-dependent potassium channel 1.3 (Kv1.3^{-/-}) are thin without caloric restriction and have low levels of circulating glucose and leptin (Fadool *et al.* 2004; Xu *et al.* 2004; Tucker *et al.* 2008, 2012a; Thiebaud *et al.* 2014). Kv1.3 channels are dampeners of neuronal excitability but have also been shown to be important in control of energy homeostasis (Upadhyay *et al.* 2013). When Kv1.3^{-/-} mice are placed on fatty diets, they are resistant to DIO and the diet does not cause a loss in olfactory discrimination despite the fact that they still exhibit structural loss of OSNs and their associated axonal projections (Tucker *et al.* 2008, 2012a; Thiebaud *et al.* 2014). Because genetically obese MC4R^{-/-} mice gain adiposity on a control diet (CF), but do not lose OSNs, and the resistance of obesity in Kv1.3^{-/-} mice maintained on moderately high-fat (MHF) diet does not prevent loss of OSNs, we hypothesized that loss of olfactory structure and function could be the result of the consumption of dietary fat or excess nutrition.

To test the idea that increased fat in the diet was the culprit for olfactory losses, we established a pattern of pair-feeding whereby mice were maintained on isocaloric diets for 5 months but challenged with diets consisting of different fat percentages. To test our hypothesis that adiposity was not a prerequisite for loss of sensory structures in the olfactory system, we used mice with an OR-linked genetic reporter to visualize circuitry changes in response to fat in the diet while monitoring glucose clearance ability (prediabetes), body fat deposition, ingestive behaviours, select inflammatory markers and energy metabolism. Even though male mice that were pair-fed the MHF diet did not gain adiposity nor total body weight over that of MHF *ad libitum* fed mice and were able to clear a glucose challenge the same as control-fed mice, they still exhibited loss of OSNs and associated axonal projections. Interestingly, our data showed a sexual dimorphism, in that we were

unable to significantly induce DIO in female mice. Even though female mice exhibited an inability to clear glucose (prediabetes) when fed MHF *ad libitum*, they did not gain adiposity. Moreover, isocalorically maintained female mice consuming excess fat via MHF diets were not prediabetic, but still retained loss of OSNs and associated axonal projections. Exercise is well-known to reduce adiposity and associated inflammation brought on by DIO. We then tested the secondary hypothesis that voluntary running could reverse the deleterious effects of the structural losses of olfactory neurons. Albeit improving other health metrics in the mice, including total EE, glucose tolerance, adipose deposition and body weight, exercising while consuming an *ad libitum* fatty diet still precipitated loss of OSNs and associated axonal projections. These results suggest that the long-term macronutrient imbalance of a fatty diet can drive anatomical loss in the olfactory system regardless of total EE.

Methods

Sequence of experiments and animal care

Different series of experiments were performed on transgenic lines of mice (to include modified diet, isocaloric feeding paradigms, serum chemistry, fat determination, glucose sensitivity, food intake, access to voluntary running, olfactory behaviours and/or systems physiology metabolic parameters) prior to final histological processing to determine any changes in olfactory circuitry and structure. The sequence of experimental events is diagrammed in Fig. 1 for ease of reference, and the associated methods are partitioned into two main cohorts or experiments, accordingly. Mice were maintained on either a CF diet consisting of Laboratory Rodent Diet 5001 (LabDiet, St Louis, MO, USA; 28.05% kcal protein, 59.81% kcal carbohydrate and 13.5% kcal fat; <https://www.labdiet.com/Products/StandardDiets/Rodents/index.html>) or a Moderately High-fat Condensed Milk Diet (MHF; cat. no. D12266B, from Research Diets, Inc., New Brunswick, NJ, USA; 16.8% kcal protein, 51.4% kcal carbohydrate and 31.8% kcal fat; <https://researchdiets.com/formulas/d12266b>). Mice were weaned at 4 weeks and then randomly assigned to dietary/treatment group, which was initiated within 1 week. Littermates were assigned different dietary/treatment groups within an experiment to minimize any varying effects of maternal behaviour.

Ethical approval

All mice were housed in the animal vivarium at Florida State University (FSU) in conditions compliant with institutional requirements, the National Institutes of

Health (NIH), and the American Veterinary Medicine Association (AVMA). All performed procedures were approved under the FSU Animal Care and Use Committee protocol nos 1733 and 202000036. In preparation for histology, mice were anaesthetized with a mixture of ketamine (100 mg/kg body weight) and xylazine (10 mg/kg body weight) prior to intracardial perfusion with 4% paraformaldehyde and euthanasia by decapitation (AVMA Guidelines on Euthanasia, June 2007). All authors understood the ethical principles that *The Journal of Physiology* operates under, and the work complied with the animal ethics checklist reported by Grundy (2015).

Experiment 1: pair feeding

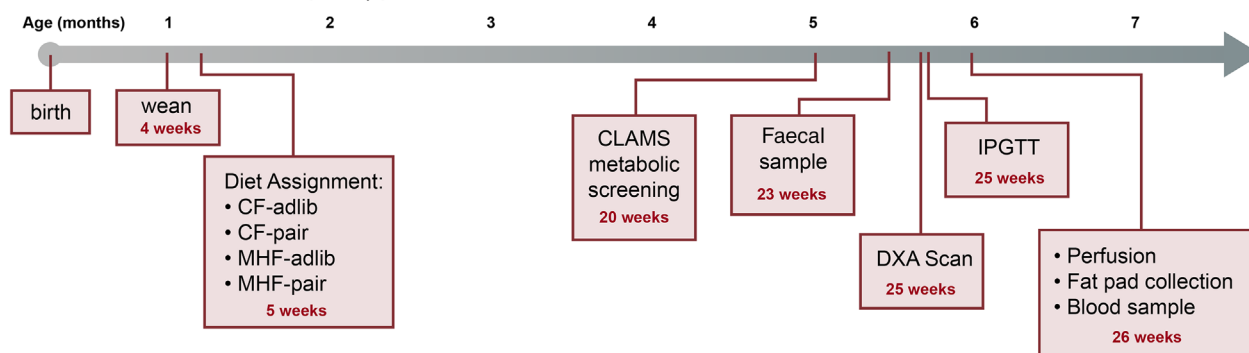
Mouse husbandry and lines. To investigate the impact of dietary fat on the olfactory system, a transgenic line of mice with a genetic marker for OSNs expressing the odorant receptor *Olfr160* was used. This mouse

line (*M72tauLacZ*; deposited at The Jackson Laboratory, Bar Harbor, ME, USA – stock number 006596, <https://www.jax.org/strain/006596>, RRID: IMSR_JAX:006596) allows visualization of the *Olfr160*-expressing OSNs via production of an indigo by-product in the cells following β -galactosidase histology (Zheng *et al.* 2000; Zapiec & Mombaerts, 2015). Upon weaning, mice were individually housed in conventional style mouse cages with open wire bar lids. Mice were maintained on a 12 h/12 h light–dark cycle and allowed *ad libitum* access to water.

Dietary treatment. *M72tauLacZ* mice of both sexes were randomly assigned to one of four treatment groups. Pair feeding, a feeding protocol in which the food consumption for experimental groups of mice is isocalorically matched to that of a control group, was manually maintained for 5 months (Fig. 1, experiment 1). In this design, the first group, the CF-maintained mice, was allowed food access *ad libitum* (CF adlib). The second group of mice were maintained on the CF diet, but each day were provided

Experiment 1:

Pair-feeding – *M72tauLacZ* (♂+♀)



Experiment 2:

Diet/Exercise → OSNs – *M72tauLacZ* (♂ only)

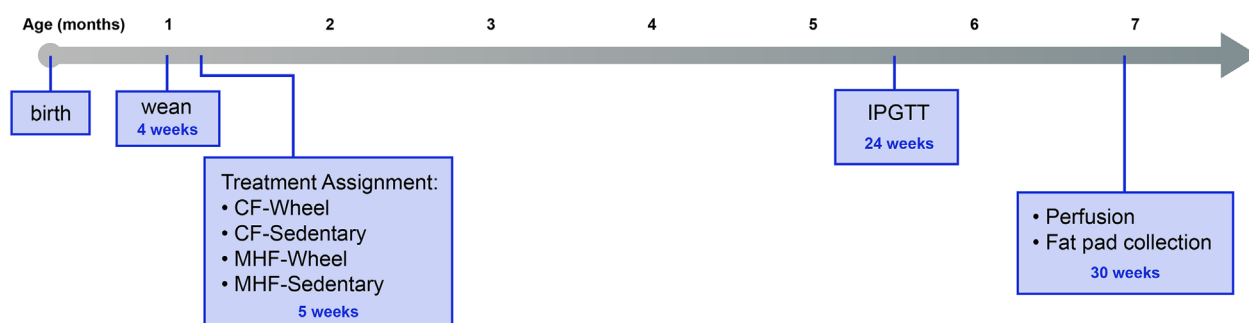


Figure 1. Experimental timelines for pair-feeding treatment (experiment 1) and voluntary exercise (experiments 2) in transgenic lines of mice with olfactory reporters

Experiment 1 (red): timeline for experiments performed using male and female *M72tauLacZ* mice that were maintained on isocaloric diets of differing fat content (pair fed). Experiment 2 (blue): timeline for experiments performed using male *M72tauLacZ* mice that were allowed access to voluntary running wheels and diets of differing fat content (diet/exercise). Histology of the main olfactory epithelium and olfactory bulb was performed for both experiments.

with an amount of food calorically equivalent to the food consumed by the respective matched CF adlib mouse the previous day (CF pair fed). The third group was MHF-maintained mice that were allowed food access *ad libitum* (MHF adlib), but of higher fat content (CF: 13.5 vs. MHF: 31.8% of kcal from fat). The fourth group (MHF pair fed) was similarly maintained on the MHF diet, but their daily food allotment was calorically equivalent to the food consumed by the matched CF adlib mouse. For the purposes of our study designs, an isocaloric diet is one in which mice consume equivalent daily calories (also known as yoked) but the diets contain differential fat percentages (CF and MHF pair diets), and an obesogenic diet is one in which the total amount of food leads to obesity or the deposition of excess adipose stores (MHF adlib). Daily body weights and food intake were collected over the 5-month treatment period and daily isocaloric feeding was calculated based upon company-reported kilocalories (CF: 3.35 kcal/g, MHF: 4.41 kcal/g). Food consumption was carefully monitored and the isocaloric design did not induce food-restricted patterns of eating.

Indirect calorimetry. To assess modulation of whole-body metabolism due to chronic participation in isocaloric diets of varying fat composition, the mice were temporarily transferred to individual metabolic chambers at 5 months of age (Fig. 1, experiment 1). Mice were acclimated to metabolic chambers for 2 days prior to systems physiology measurement. Oxygen consumption (\dot{V}_{O_2} ; ml/kg/h), carbon dioxide production (\dot{V}_{CO_2} ; ml/kg/h), respiratory exchange ratio (RER), locomotor activity, food intake (kcal) and water consumption were tracked for ~5 days using the Comprehensive Laboratory Animal Monitoring System (CLAMSTM; Columbus Instruments, Columbus, OH, USA). Metabolic data were analysed as the mean value over a continuous 72-h interval acquired in the 5-day experimental window, sorted by light or dark cycle. During the period in the CLAMS, mice had *ad libitum* access to water, but food continued to be isocalorically administered as previously described. Food and water were delivered using overhead feeders attached to specialized electronic balances that monitored both disturbance and decrease in mass. A threshold of at least 10 s of feeder disturbance and a minimum loss of 0.03 g of chow was required for a recorded meal bout. \dot{V}_{O_2} and \dot{V}_{CO_2} were normalized with respect to body weight in kilograms. RER was calculated as $\dot{V}_{CO_2}/\dot{V}_{O_2}$. EE was calculated using the Lusk equation ($3.815 + 1.232 \times \text{RER}$) $\times \dot{V}_{O_2}$ (Lusk & Du Bois, 1924). Locomotor activity was continuously measured using optical beams along the *x*-axis of the cage (Columbus Instruments). Consecutive photo beam breaks were scored as ambulatory movement. Indirect calorimetry data were recorded in intervals using Oxymax software (Columbus Instruments). Each interval

measurement represented the average value during a 30 s sampling period per cage.

Body weight and body fat. Body weight was measured and recorded daily. To determine body composition, mice underwent a dual-energy X-ray absorptiometry (DXA) scan at ~5.5 months of age (Fig. 1, experiment 1). Mice were anaesthetized with a mixture of ketamine (100 mg/kg body weight) and xylazine (10 mg/kg body weight) and scanned whole-body in the prone position (GE Lunar iDXA; GE Healthcare, Milwaukee, WI, USA). Access to the iDXA equipment was lost prior to completion of the experiment. Thus, some mice were scanned using an EchoMRI machine (EchoMRI LLC, Houston, TX, USA) instead to determine body composition. Upon termination, we also manually excised and weighed adipose tissue from the carcasses of the mice. A researcher blinded to the treatment group collected the interscapular brown, mesenteric, retroperitoneal, subcutaneous (sub-sample on right side), and epididymal (male) or endometrial (female) fat pads and weighed them separately as previously performed (Tucker *et al.* 2012a).

Glucose tolerance. An intraperitoneal glucose tolerance test (IPGTT) was performed on the mice between 5 and 6 months of age (Fig. 1, experiment 1). Mice were fasted for 6 h starting at the beginning of the dark phase, and then were injected with a volume of 25% glucose solution equivalent to 2 g of glucose per kg of lean body mass (as determined previously via DXA or EchoMRI). A small incision was made on the tail and blood samples were collected with a Contour Next Blood Glucose Monitoring System (Ascensia Diabetes Care US, Inc.; Parsippany, NJ, USA) paired with Contour Next Blood Glucose Test Strips (Ascensia) to determine blood glucose levels at baseline (prior to injection) and at set time points 15, 30, 60, 90 and 120 min following the injection. The area under the resulting curve was integrated (iAUC) per mouse and compared across treatment groups.

Solutions and reagents. Solutions used for tissue preparation or visualization of β -galactosidase reaction product, namely, phosphate-buffered saline (PBS), Buffer A, Buffer B and Buffer C, were made as described previously (Biju *et al.* 2008; Thiebaud *et al.* 2014). PBS contained (mM): 137 NaCl, 2.7 KCl, 10 Na₂HPO₄ and 1.8 KH₂PO₄. Buffer A contained 0.1 M phosphate buffer, 2 mM MgCl₂ and 5 mM EGTA. Buffer B contained 0.1 M phosphate buffer, 2 mM MgCl₂, 0.01% sodium deoxycholate and 0.02% Nonidet P40. Buffer C consisted of Buffer B with 5 mM potassium ferricyanide, 5 mM potassium ferrocyanide and 1 mg/ml X-gal. Slides used for collection of tissue sections were gel coated with a solution containing 1% w/v gelatin and 2 mM chromium

potassium sulfate. X-gal was purchased from Research Products International Co. (Mt Prospect, IL, USA). All salts were obtained from Sigma (St Louis, MO, USA) or Thermo Fisher Scientific (Waltham, MA, USA).

β -Galactosidase histology and imaging. Mice were anaesthetized using a mixture of ketamine and xylazine (as above). A toe pinch test was used to ensure the state of anaesthesia prior to intracardiac perfusion with PBS followed by 4% w/v paraformaldehyde (PFA)/PBS for 5 min each. Following the perfusion, the heads were removed and placed in 4% PFA/PBS at 4°C for 4 h. The skulls were then rinsed in PBS for 15 min, replacing the PBS every 5 min. The skulls were next decalcified by transferring them into 0.3 M EDTA in PBS for approximately 5 days. The skull and remaining tissues were carefully removed leaving the brain with the olfactory epithelium intact. Caution was used when removing the upper incisors because they run along the length of the olfactory epithelium and poor technique during their removal can damage the tissue. The exposed olfactory bulbs and olfactory epithelium were then stained to visualize β -galactosidase-expressing Olfr160-positive OSNs (Biju *et al.* 2008; Thiebaud *et al.* 2014). Briefly, the tissues were washed with Buffer A for 5 min and then again for 25 min, followed by two 5-min washes with Buffer B. The tissues were then incubated in Buffer C for 10 h followed by 0.1 M phosphate buffer to stop the reaction.

The olfactory bulb whole-mounts were imaged using a Leica MZ FLIII stereomicroscope (Leica Microsystems, Buffalo Grove, IL, USA) outfitted with a Zeiss AxioCam paired with AxioVision software (Carl Zeiss Microimaging, Jena, Germany). The pixel density of the Olfr160 glomerulus and its associated axonal projections for each bulb pair were estimated using the open-source image processing software Fiji (Schindelin *et al.* 2012). The whole-mount images were converted to greyscale and a threshold was applied that differentiated stained OSN projections from unstained tissue. The threshold was variable for each converted greyscale image but was adjusted to reflect the staining in the original image as closely as possible. Application of the threshold instructed the software to consider all pixels darker than the threshold as black and those lighter as white. Then the regions of interest (ROI) were drawn using the freehand selection tool around the pair of lateral glomeruli and their associated projections, quantifying the number of total black pixels for the olfactory bulb pair per mouse. The medial glomeruli were not measured due to the difficult angle of their position casting a shadow in the whole-mount images when pixel converting.

Following whole-mount imaging, the olfactory bulbs (with olfactory epithelium still attached) were cryoprotected in 10% w/v sucrose/PBS followed by 30%

w/v sucrose/PBS. The tissues were incubated at 4°C in each sucrose solution until they sank to the bottom of the histology tube. The cryoprotected tissues were then frozen in O.C.T. embedding medium (Thermo Fisher Scientific) and stored at -80°C . The tissues were cryosectioned coronally from the start of the olfactory epithelium through the end of the olfactory bulbs at $16\ \mu\text{m}$ thickness on a CM1860 cryostat (Leica) with the chamber temperature set at -20°C . Sections were collected on gelatin-coated Superfrost slides (cat. no. 48311-601, VWR International, Radnor, PA, USA) and stored at -20°C until use. The sectioned tissue was stained again, repeating the same procedure as described for the whole mounts. The slides were returned to room temperature, and washed with Buffer A for 5 and 25 min, and then Buffer B twice for 5 min. The slides were then incubated in Buffer C with a $2\times$ higher concentration of X-gal for 48 h as opposed to the procedure above. This resulted in strong staining without the need for counterstaining so that the OSNs could be easily identified and manually counted. The Olfr160-expressing OSNs were visualized and enumerated manually via light microscopy with an Axiovert 135 (Zeiss). The number of Olfr160-positive OSNs was summed across the entire epithelium per mouse. Each mouse was counted with the investigator blind to the treatment of the animal.

Faecal sampling and corticosterone quantification. Mice were provided with a clean cage at the onset of the dark phase. At the conclusion of the dark phase and the beginning of the light phase, the mice were provided with a second clean cage. At the conclusion of the light phase, the mice were transferred again to a third clean cage. The dark phase and light phase cages were emptied individually, and all faecal matter was collected via manual survey through the bedding. Each 12 h faecal sample was stored at -80°C until processing. Corticosterone was quantified using a Corticosterone Competitive ELISA Kit (cat. no. EIACORT; Thermo Fisher Scientific). Steroid extraction, sample preparation and the ELISA were performed according to the manufacturer's recommended protocol.

Serum sampling and cytokine quantification. During termination by intracardiac perfusion, a blood sample was taken from each mouse. Prior to infusion of PBS, a 20G needle was inserted into the caudal vena cava from which blood was collected. The blood was allowed to clot at room temperature for ~ 15 min. The samples were centrifuged at $735\ \text{g}$ at 4°C for 10 min and the supernatant was collected and stored at -20°C until processing. Interleukin 6 (IL-6) and tumour necrosis factor (TNF) were quantified using a Mouse IL-6 ELISA Kit (cat. no. KMC0061; Thermo Fisher Scientific) and Mouse

TNF ELISA Kit (cat. no. 88-7324-22; Thermo Fisher Scientific), respectively. Sample/standard preparation and the ELISAs were performed according to the company's recommended protocol.

Statistical analysis. Prior to performing any statistical comparisons, data were first analysed with the Dixon's Q-test to identify any outliers. Then data were checked for normal distribution and homogeneity of variance using the F_{\max} test. Analysis of data collected in experiment 1 did not identify any outliers nor did any collected data violate homogeneity of variance (fail the F_{\max} test). Mean body weight, fat pad weight, food intake, iAUC for the glucose clearance curves, pixel counts for Olfr-160 glomeruli and axonal projections in whole-mount images, manual counts of Olfr-160-positive OSNs, faecal corticosterone levels, and serum IL-6 and TNF concentration were each analysed using a one-way analysis of variance (ANOVA) with dietary treatment as the factor at the 95% confidence level ($\alpha \leq 0.05$). Metabolic data from the CLAMS were analysed using a one-way ANOVA with dietary treatment as the factor at the 95% confidence level ($\alpha \leq 0.05$). Comparison of metabolic data across light vs. dark cycle within dietary treatment was analysed using a one-tailed, paired Student's *t*-test ($\alpha \leq 0.05$). Body weight over age measurements were analysed with a two-way repeated measures analysis of variance (RM-ANOVA) using dietary treatment and time as factors. For the ordinary and RM-ANOVA tests, the Tukey or Bonferroni method for multiple comparison testing was used as the *post hoc* analysis to make mean-wise comparisons between treatments. Males and females were analysed as separate cohorts. All reported values in the text and figures are means \pm standard deviation (SD). Sample sizes are reported as individual data points in the graphs and represent number of mice. Individual *F*-statistic, and *P*-values are reported for each experiment within the corresponding graph as described in the Results section. Statistical tests were performed using GraphPad Prism 9 (GraphPad Software, San Diego, CA, USA) while the graphs and figures were produced using Origin v8 (OriginLab Corp., Northampton, MA, USA), Adobe Photoshop CS4 (Adobe, Inc., San Jose, CA, USA), and the open-source graphics editing software Inkscape (<https://inkscape.org/release/inkscape-1.1/>).

Experiment 2: voluntary exercise effect on OSNs

Mouse husbandry and lines. To investigate the interactive effects of diet composition and wheel running on the olfactory system, M72*tau*LacZ male mice were weaned to larger cages (47 cm L \times 23.8 cm W \times 20.3 cm H) to accommodate running wheel equipment (Fig. 1, experiment 2). Mice were maintained on a 12/12 h

light–dark cycle and allowed *ad libitum* access to food and water.

Voluntary wheel running. For the voluntary running experiments, M72*tau*LacZ mice were randomly assigned to either the CF or the MHF diet. Within each diet group, the mice were further divided into either a voluntary exercise (VEx) or a sedentary treatment (SED). Mice assigned to the VEx treatment received *ad libitum* access to a Vertical Wireless Running Wheel (Med Associates, Inc., St Albans, VT, USA) as previously described (Chelette *et al.* 2019). Briefly, a wheel sensor was placed on top of the wire bar lid with plastic manifolds extending into the cage that held the wheel above the bedding to allow for rotation. Mice were provided with a clean running wheel biweekly that was lubricated with odourless, tasteless, non-caloric silicone oil. The wheel running data were collected using the Wheel Manager software program (Med Associates, Inc., <https://www.medassociates.com/product/wheel-manager/>), which archived the data every 30 s. Upon conclusion of data collection, the running data were exported through the Wheel Analysis software program (Med Associates, Inc.). The data were exported, organized and analysed using a combination of Wheel Analysis (Med Associates), Microsoft Excel, and R (R Core Team, Vienna, Austria) software.

Body weight and body fat. Body weight was measured and recorded weekly. Following termination, the mesenteric, retroperitoneal, subcutaneous and epididymal fat pads were removed from the carcasses and weighed collectively. Brown fat was not collected.

Glucose tolerance. An intraperitoneal glucose tolerance test (IPGTT) was performed on mice between 5 and 6 months of age, as in experiment 1, the exception being that mice in this cohort were fasted for 12 h starting at the beginning of the light phase.

Termination and histology. Termination and fixation by intracardiac perfusion as well as the β -galactosidase staining on whole mounts and cryosectioned tissues were performed the same as in experiment 1.

Statistical analysis. Prior to performing any statistical comparisons, data were first analysed with the Dixon's Q-test to identify any outliers. Then data were checked for normal distribution and homogeneity of variance using the F_{\max} test. Analysis of data collected for experiment 2 did not identify any outliers nor did collected data violate homogeneity of variance (fail the F_{\max} test). Mean body weight, adipose tissue weight, iAUC for the glucose clearance curves, pixel counts for whole-mount images

and Olf160-positive OSN counts were analysed, and the data were presented in the same way as experiment 1 with the notable exception that only males were used for these experiments. Running distance, time and velocity were compared between CF and MHF maintained mice using Student's *t*-test at the 95% confidence level ($\alpha \leq 0.05$).

Results

Mice maintained on an isocaloric diet containing MHF retain loss of axon projections

To test whether a modified diet containing fat could perturb the abundance and circuitry of OSNs, *M72tauLacZ* mice were challenged for 5 months with

MHF diet, which was either provided *ad libitum* (adlib) or isocalorically matched to that of a control-fed mouse (pair). The density of axonal projections observed by whole-mount imaging of the β -galactosidase staining of Olf160 axons was captured by thresholding to a fixed level – on a black and white scale – and then computing total pixel density for the lateral Olf160 glomerulus in the right and left olfactory bulb (Fig. 2A and B). The goal of this feeding protocol was to maintain mice on MHF diets without an induction of increased body weight or adiposity, and then observe the extent of any olfactory anatomical perturbations due to dietary content. As anticipated from earlier investigations where mice were challenged with DIO (Thiebaud *et al.* 2014), mice that had *ad libitum* access to the MHF diet (MHF adlib)

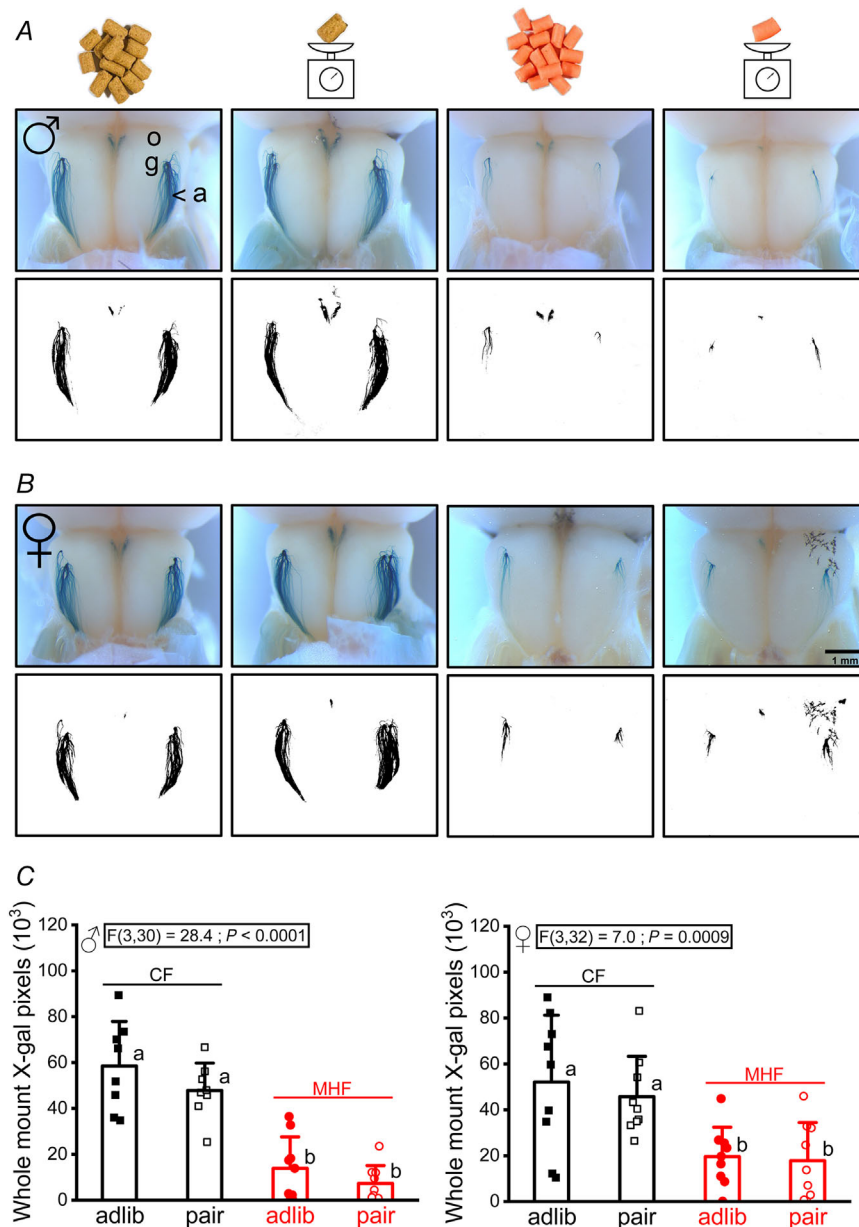


Figure 2. Reduction of Olf160 axonal projections in mice following consumption of high fat diet

A and B, representative whole-mount images of olfactory bulbs following β -galactosidase histological staining of Olf160-expressing olfactory sensory neurons (OSNs) from male (A) and female (B) *M72tauLacZ* mice following dietary treatments. Images from left to right: control diet *ad libitum* (brown food symbol), control diet isocaloric pair-fed (brown food and scale symbol), moderately high-fat diet *ad libitum* (pink food symbol), moderately high-fat diet isocaloric pair-fed (pink food and scale symbol). Corresponding greyscale images were used for pixel determination in (C). o, olfactory bulb; g, glomerulus; a, Olf160 axonal projections. C, bar graph of total Olf160 axon projections vs. diet treatment in male (left) and female (right) mice. Symbols represent individual mice sampled from left to right: CF adlib, control diet *ad libitum* (■); CF pair, control diet isocaloric pair fed (□); MHF adlib, moderately high-fat diet *ad libitum* (●); MHF pair, moderately high-fat diet isocaloric pair-fed (○). Data are reported as means \pm standard deviation in this and all subsequent figures. Sample size of number of mice from left to right, male 8, 8, 9, 9; female, 9, 9, 9, 9. One-way ANOVA across treatment groups within each sex. Degrees of freedom, *F* test, and *P*-value of the ANOVA are reported in each figure panel, here and in subsequent figures. Letters indicate significantly different, Tukey's *post hoc* test corrected for multiple comparisons, $P < 0.05$.

Table 1. Pro-inflammatory cytokine production and inhibitory regulator in response to dietary treatment

Assay target	Sample	CF adlib	CF pair	MHF adlib	MHF pair	P
Males						
TNF (pg/ml)	Serum	26.1 ± 20 (7) [a]	28.4 ± 16.6 (7) [a]	78.4 ± 42 (9) [b]	84.2 ± 31.6 (8) [b]	0.0005
IL-6 (pg/ml)	Serum	71.4 ± 93.9 (5)	36.8 ± 25.1 (4)	72.4 ± 55.2 (5)	67.8 ± 102.4	0.9000
CORT (pg/ml)	Faecal					
12 h dark		4301 ± 1494 (5)	4355 ± 688 (5)	3950 ± 678 (6)	4901 ± 1003 (6)	0.9200
12 h light		4342 ± 1370 (5)	4236 ± 1493 (5)	4130 ± 625 (6)	3989 ± 1083 (6)	0.9600
Females						
TNF (pg/ml)	Serum	26.1 ± 11 (7) [a]	31.1 ± 16.4 (9) [a]	67.24 ± 29 (8) [b]	71.2 ± 28.6 (9) [b]	0.0003
IL-6 (pg/ml)	Serum	41.6 ± 43.3 (6)	69.3 ± 64.5 (6)	116.5 ± 59.6 (5)	81.4 ± 64.9 (6)	0.2400
CORT (pg/ml)	Faecal					
12 h dark		4163 ± 1306 (6)	3949 ± 1602 (6)	3689 ± 380 (6)	4206 ± 1284 (5)	0.9100
12 h light		3701 ± 778 (6)	3808 ± 625 (6)	3916 ± 449 (5)	4582 ± 1052 (5)	0.2600

Mean ± SD (sample size); dietary factor: 1-way ANOVA (*P* value) with Tukey's *post hoc* test ($\alpha \leq 0.05$) [letter]. adlib, *ad libitum*; CF, control fed; CORT, corticosteroid; IL-6, interleukin 6; MHF: moderately high fat diet; pair, isocalorically fed to match CF; TNF, tumour necrosis factor α .

exhibited a significant loss of Olfr160-expressing olfactory sensory axonal projections (Fig. 2) compared with those maintained on control diets (CF adlib and CF pair fed). This loss of projections was true for both male (Fig. 2A) and female (Fig. 2B) mice, the latter of which had never been examined with respect to loss of axonal projections or OSNs attributed to fatty diet. Interestingly, mice of both sexes also lost significant Olfr160-expressing axonal projections when they consumed the same daily caloric intake as CF adlib mice but did so in the form of MHF diet (Fig. 2C; one-way ANOVA using dietary treatment as the factor, with Tukey's *post hoc* test). Here, and in all subsequent analyses using the between-subjects ordinary ANOVA, the *F*-statistic is reported with the numerator and denominator degrees of freedom (d.f.) as the number of (groups - 1) and number of (groups × sample size) - number of groups, respectively. The sample size (*n*) represents number of mice. The generated *F*-value (= $F(\text{d.f.}_{\text{numerator}}, \text{d.f.}_{\text{denominator}})$) and *P*-value are reported in each graph of the figure. The *post hoc* test is indicated by lower case letters, whereby different letters indicate significantly different group means at $\alpha \leq 0.05$. We examined both CF adlib and pair conditions to confirm that the CF pair treatment did not exhibit any degree of stress by being restrained to the caloric consumption of a pair fed animal, despite both treatment groups consuming an identical CF diet. Although the body weight and other noted metrics (see below) must always be restrained in the pair treatment by design, a collection of faecal pellets from mice in all four treatment groups failed to demonstrate significant changes in corticosterone levels (Table 1; males dark cycle, $F(3, 18) = 0.9170$, $P = 0.4525$; males light cycle, $F(3, 18) = 0.09269$, $P = 0.9631$; females dark cycle, $F(3, 18) = 0.1829$, $P = 0.9066$; females light cycle, $F(3, 18) = 1.457$, $P = 0.2597$), suggesting lack of

measurable stress hormones induced by the pair feeding regimen.

Mice maintained on an isocaloric diet containing MHF retain loss of OSNs

Because there was a significant loss of Olfr160-expressing axonal projections to their corresponding glomeruli in both the MHF diet *ad libitum* (MHF adlib) and isocaloric conditions (MHF pair), it was anticipated that there should be a concomitant loss of Olfr160 OSNs for these same treatments at the level of the epithelium. We sectioned across entire main olfactory epithelia of differentially fed mice and found a significant loss of OSN abundance regardless of whether mice consumed the MHF diet freely (MHF adlib) or whether they were restricted to the calories consumed by CF adlib mice (MHF pair) (Fig. 3; 1-way ANOVA with Tukey's *post hoc* test). This loss of OSNs was not sex dependent (Fig. 3D) and occurred in female mice despite the absence of DIO in females (see Fig. 4 and below).

Isocalorically maintained male mice consuming MHF have normal body weight, body fat and caloric intake, and have improved glucose tolerance

By taking weekly body weight measurements, we observed that the mean body weight of male mice that were allowed *ad libitum* access to MHF diet began to diverge from other dietary treatment groups at about 2 months of treatment (Fig. 4A, left). An analysis of diet and time as factors showed a significant difference of both variables as well as a diet × time interaction (Fig 4A, left; 2-way RM-ANOVA

with Tukey's *post hoc* test). *Post hoc* tests indicated an elevation of body weight in the MHF *ad libitum* treatment compared with all three other treatment groups starting at 13 weeks of age. We additionally performed comparisons of body weight, body fat, and adipose deposition at 5 months of treatment. Mice that consumed MHF *ad libitum* had significantly greater body weight (Fig. 4A, left, inset; 1-way ANOVA with Tukey's *post hoc* test), an effect that was consistent with an increase in daily and cumulative food consumption (Fig. 4B and C, left; 1-way ANOVA with Tukey's *post hoc* test). It was noteworthy that MHF pair-fed mice were not significantly different in any of these metrics from CF mice (Fig. 4A–C, left). In males, there was a strong correlation between food intake and final body weight (Fig. 4D). All male treatment groups displayed similar amounts of lean body mass (Fig. 5A, left) and the surplus body weight displayed by the male MHF *ad lib* mice correlated with significantly higher fat mass as determined by DXA and EchoMRI

(Fig. 5A, left) as well as post-termination, manual excision of fat depots (Fig. 5B, left). By analysing post mortem adipose tissue localization, we found that epididymal fat was the greatest source of adipose accumulation, but that every common source of deposition was significantly elevated in the MHF *ad lib* diet treatment for males (DXA/EchoMRI lean body mass: $F(3, 30) = 0.3$; $P = 0.86$; DXA/EchoMRI fat mass: $F(3, 30) = 8.1$; $P = 0.0004$; total weight of excised fat pads: $F(3, 30) = 28.2$; $P < 0.0001$; epididymal: $F(3, 30) = 43.8$; $P < 0.0001$; retroperitoneal: $F(3, 30) = 17.3$; $P < 0.0001$; Mesenteric: $F(3, 30) = 8.8$; $P = 0.0002$; subcutaneous: $F(3, 30) = 17.5$; $P < 0.0001$; intrascapular brown: $F(3, 27) = 9.7$; $P = 0.0002$; Fig. 5A and B, left; 1-way ANOVA with Tukey's *post hoc* test). By comparison, fat deposition for the isocalorically, pair fed MHF dietary treatment was not significantly different from that of CF *ad lib* controls (Fig. 5A and B, left; 1-way ANOVA with Tukey's *post hoc* test). In fact, none of the adipose tissue accumulations in pair fed mice (CF or

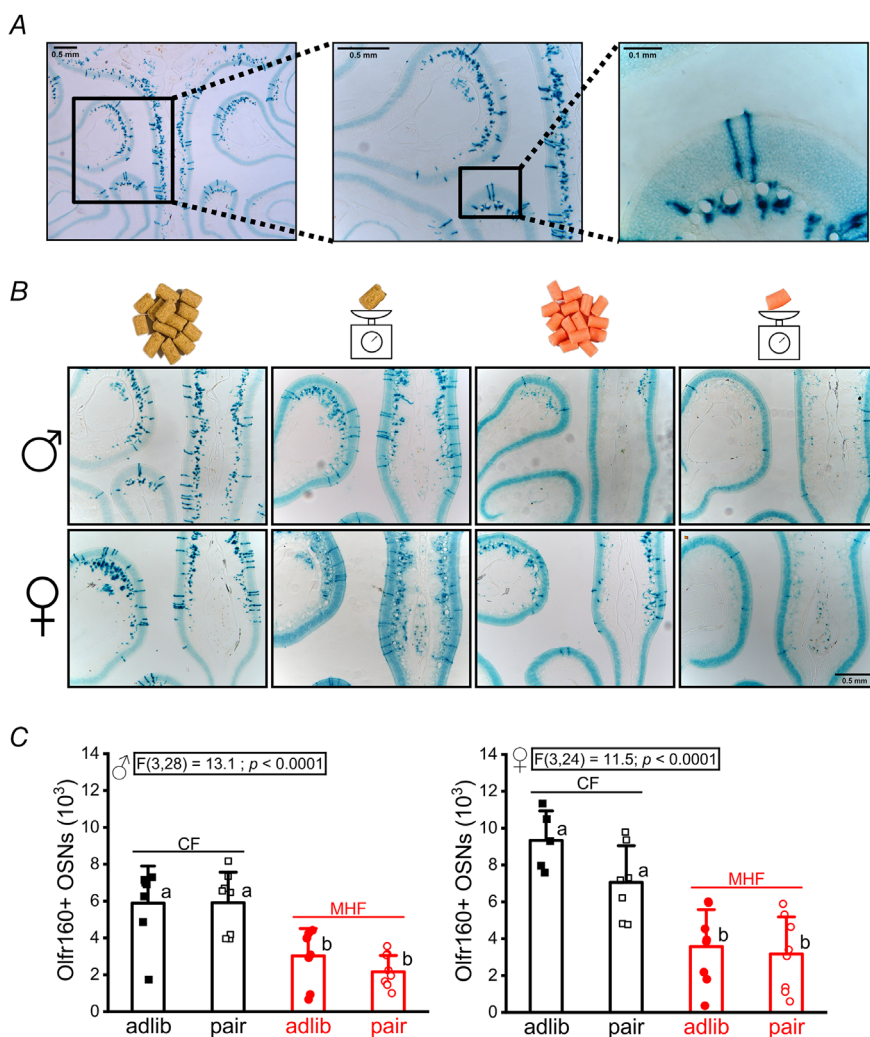


Figure 3. Reduction in number of Olfr160-expressing olfactory sensory neurons in mice following consumption of moderately high-fat diet

A, representative coronal tissue section of an olfactory epithelium (OE) at three different magnifications acquired from a M72tauLacZ male mouse maintained on a control diet *ad libitum* (CF *ad lib*). The indigo cells are Olfr160-expressing olfactory sensory neurons (OSNs). OE, olfactory epithelium; OSN, olfactory sensory neuron. B, representative images of an OE following one of the four dietary treatments in male (top) and female (bottom) mice. Scale bar: 0.5 mm. C, bar graph of the number of Olfr160-expressing OSNs vs. dietary treatment in males (left) and females (right). Notations and statistical analyses as in Fig. 2. Males: 8, 8, 8, 9; females: 6, 7, 8, 8.

MHF) were elevated above that of CF adlib controls. Male mice that consumed MHF isocalorically (pair) had body weights, food consumption, body mass and fat depots that were not significantly different from those of CF adlib or pair treatments (Figs 4 and 5). Interestingly, despite

a lack of changes in body weight, food consumption and adiposity, the MHF isocaloric treatment did elicit an intermediate change in glucose sensitivity compared with MHF adlib and CF adlib treatment conditions (Fig. 5C).

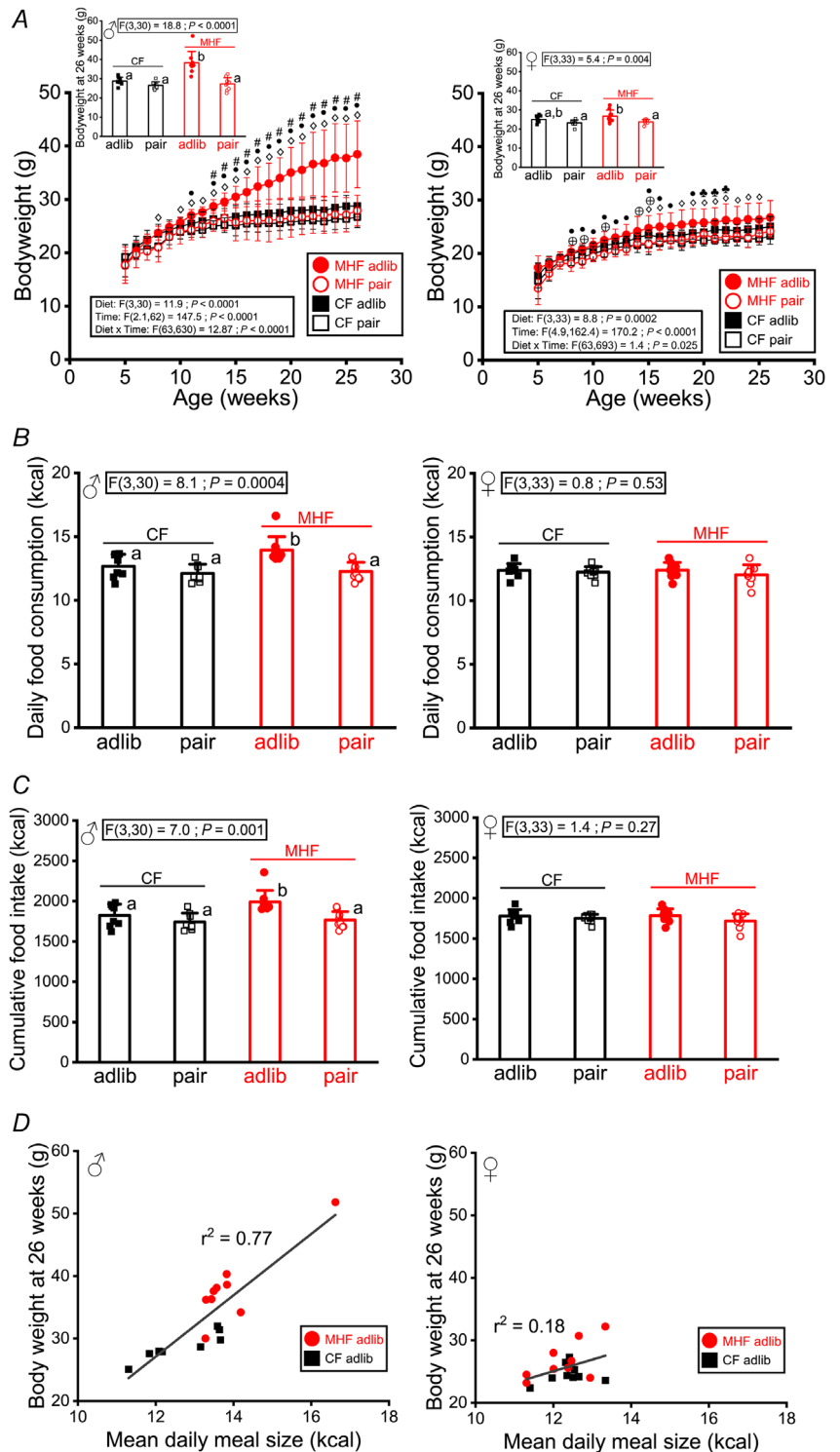


Figure 4. Male mice selectively increase body weight and food intake when dietary fat is consumed *ad libitum* rather than isocaloric pair-fed

A, line graph of body weight for male (left) and female (right) M72*tau*LacZ mice vs. age following dietary treatment initiated at 5 weeks of age; two-way RM-ANOVA; symbols indicate significant group differences for dietary factor as determined by Tukey's *post hoc* test ($P < 0.05$) as follows: # indicates MHF adlib > CF adlib; • indicates MHF adlib > MHF pair; ◊ indicates MHF adlib > CF pair; ⊕ indicates CF adlib > MHF pair; ♣ indicates CF adlib > CF pair. Inset: bar graph of body weight at 26 weeks of age vs. dietary treatment group. One-way ANOVA; letters indicate significantly different Tukey's *post hoc* corrected for multiple comparisons, $P < 0.05$. B and C, bar graph of daily food consumption (B) and cumulative food intake (C) over the duration of the experiment for male (left) and female (right) mice. One-way ANOVA with Tukey's *post hoc* test, $P < 0.05$. D, scatterplot fitted by linear regression demonstrating degree of correlation (r^2) between daily meal size and body weight at 26 weeks of age in male (left) and female (right) mice. Notation as in Fig. 2. Males: 8, 8, 9, 9; females: 9, 10, 9, 9.

Female mice are not responsive to DIO, yet do exhibit glucose insensitivity with MHF adlib treatment, which improves with isocaloric diet

In contrast to male mice, female mice showed a different pattern of body weight gain with dietary treatment. An analysis of diet and time as factors did show a significant difference of both variables as well as a diet × time interaction; however, *post hoc* tests indicated that MHF *ad libitum* treatment was not different from that of CF mice (Fig. 4A, right; 2-way RM-ANOVA with Tukey's *post hoc* test), signifying a resistance to DIO. In fact, CF adlib mice had body weights that were greater than both pair-fed treatments (CF and MHF), and only the MHF adlib mice had body weights that were greater

than that of the MHF pair-fed mice. When additionally performing comparisons of body weight, body fat and adipose deposition at 5 months of treatment, we found that female mice did not have significant changes in body weight for any of the dietary treatments compared with CF mice (Fig. 4A, right, inset; 1-way ANOVA with Tukey's *post hoc* test), nor did they demonstrate any changes in food intake (Fig. 4B and C, right), correlation of body weight and meal size (Fig. 4D, right), or changes in lean/fat tissue deposition or adiposity (Fig. 5A and B, right). Nonetheless, female mice, like males, did demonstrate a failure to clear glucose following *ad libitum* access to MHF, which was also intermediately affected when the MHF was isocalorically consumed (Fig. 5C, right; 1-way ANOVA with Tukey's *post hoc* test).

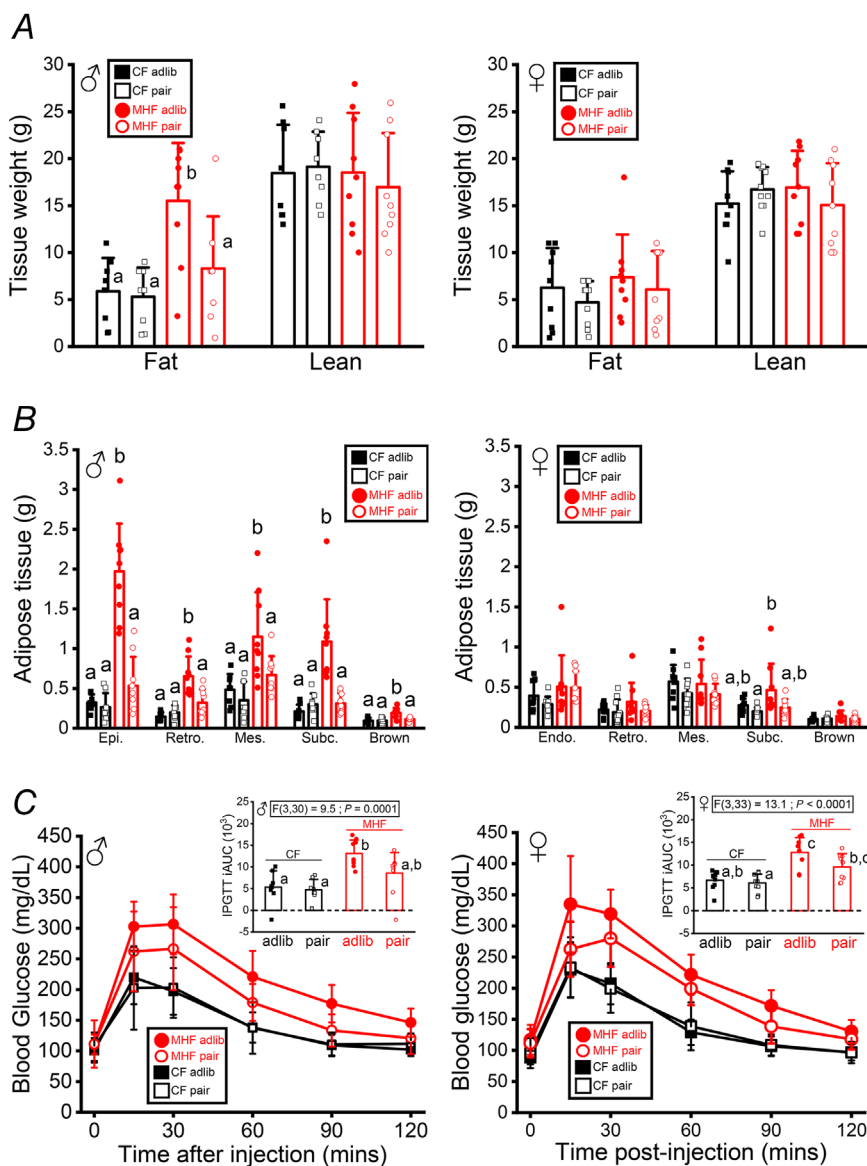


Figure 5. Male, but not female, mice increase adiposity when dietary fat is consumed *ad libitum* rather than isocaloric pair-fed. Both sexes demonstrate an impaired glucose clearance when dietary fat is consumed *ad libitum*, and an intermediate impairment when consumed isocalorically
 A, bar graph of fat and lean tissue mass vs. dietary treatment in male (left) and female (right) M72*tau*LacZ mice. B, bar graph of excised fat pad weight vs. dietary treatment; male (left), female (right). Epi, epididymal; Retro, retroperitoneal; Mes, mesenteric; Subc, subcutaneous; Brown, intrascapular brown; Endo, endometrial. C, line graph of the plasma glucose concentration during the IPGTT; inset: bar graph of the integrated area under the curve (iAUC). Notation and statistical analyses as in Fig. 2. Males: 8, 8, 9, 9; females: 9, 10, 9, 9.

Changes in serum pro-inflammatory cytokine production

Obesity is associated with low-grade inflammation, and therefore we investigated whether there might be changes in cytokines in the plasma of MHF adlib or MHF pair-fed animals. While there was not a significant change in the levels of interleukin 6 (IL-6), there was a significant elevation of tumour necrosis factor α (TNF α) in mice administered MHF diets regardless of state of adiposity (Table 1). Elevation of this adipocyte-derived chemokine is associated with decreased glucose clearance and increased insulin resistance, so it was interesting that we found a significant elevation of TNF α in both male and female mice, especially given the resistance of DIO in the latter, which retained, however, a state of prediabetes with MHF diets.

Differences in EE and RER between mice with *ad libitum* vs. a pair fed eating regime

Despite there being sex-specific differences in sensitivity to DIO in the mice, males and females responded similarly with respect to changes in EE and fuel utilization (RER) when comparing these metrics across *ad libitum* vs. a pair fed eating regime. Both male and female mice exhibited a significant difference in EE during the light cycle (Fig. 6A; 1-way ANOVA with Bonferroni's *post hoc* test). Mice maintained on *ad libitum* MHF diet had an elevated EE over that of CF pair-fed mice, independent of sex. During the dark cycle (Fig. 6B; 1-way ANOVA with Bonferroni's *post hoc* test), this effect was less pronounced, and did not reach significance for males. Fuel utilization, or RER, was significantly different across dietary treatments in both male and female mice, and across both light

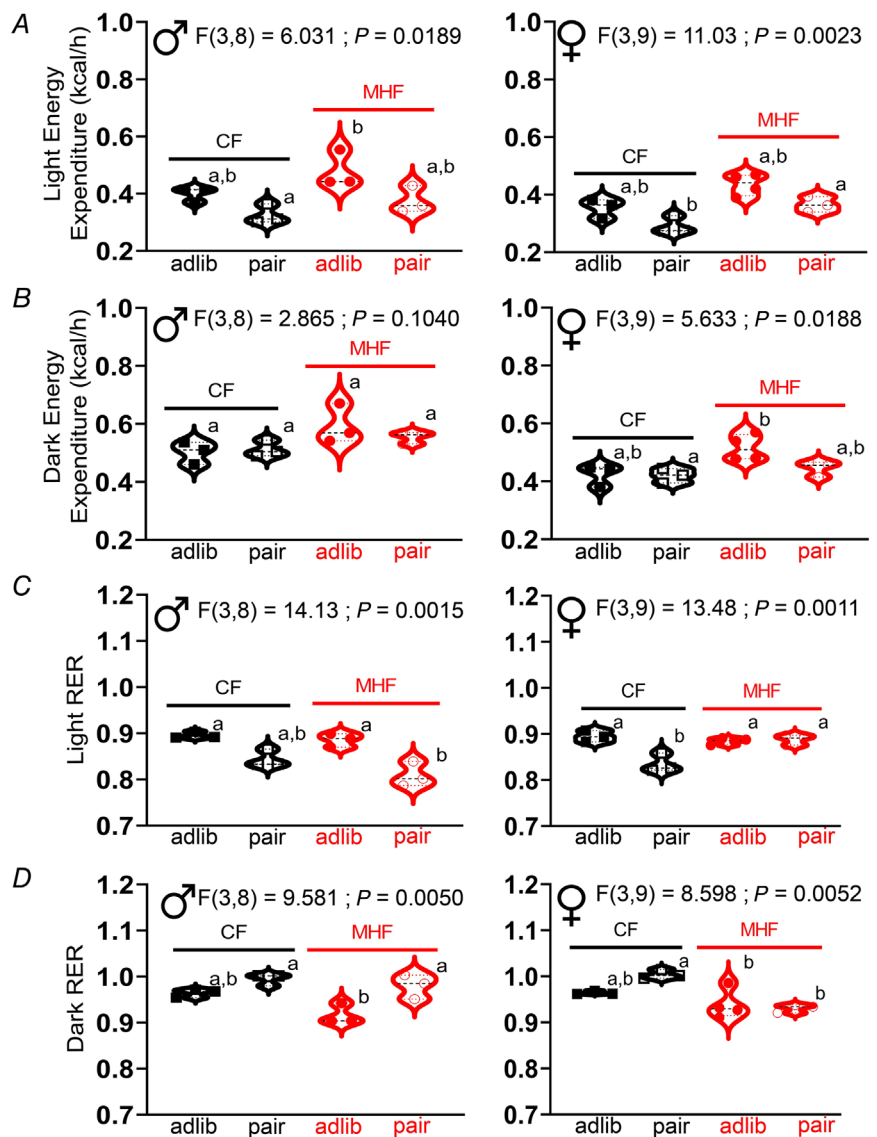


Figure 6. Changes in energy expenditure (EE) and respiratory exchange ratio (RER) measured following fat and pair-fed diet treatments

A and B, violin plot of the energy expenditure vs. dietary treatment in male (left) and female (right) M72tauLacZ mice during the light (A) and dark (B) cycle. C and D, same as A and B but for RER. Plotted are individual mice, with black dashed line (median) and dotted lines (top and lower quartile). Data represent the 12 h mean of three consecutive light or dark cycles following an initial 2-day acclimation period to the CLAMS metabolic chambers. One-way ANOVA, letters indicate significantly different Bonferroni's *post hoc* test corrected for multiple comparisons, $P < 0.05$.

Table 2. Metabolic properties in male mice in response to dietary treatment for males

Metabolic property	CF adlib	CF pair	MHF adlib	MHF pair	P
Body weight (g)	30.4 ± 1.4 (3)	27.6 ± 1.8 (3)	40.1 ± 11.1 (3)	31.0 ± 3.1 (3)	0.0745
Water intake (g)					
12 h dark	4.4 ± 0.7 (3) [a]	6.5 ± 0.8 (3) [b]	2.7 ± 0.8 (3) [a]	4.0 ± 0.7 (3) [a]	0.0014
12 h light	1.2 ± 0.1 (3) [a]*	2.2 ± 0.1 (3) [b]**	1.2 ± 0.2 (3) [a]*	0.6 ± 0.1 (3) [c]**	<0.0001
Caloric intake (kcal)					
12 h dark	15.7 ± 1.0 (3)	15.0 ± 0.9 (3)	28.6 ± 0.9 (3)	18.7 ± 10.5 (3)	0.7549
12 h light	6.1 ± 2.4 (3)*	1.6 ± 0.3 (3)***	10.4 ± 6.9 (3)	5.2 (2)	0.1844
Energy expenditure (kcal/h)					
12 h dark	0.50 ± 0.04 (3)	0.51 ± 0.03 (3)	0.59 ± 0.07 (3)	0.55 ± 0.02 (3)	0.1040
12 h light	0.40 ± 0.03 (3) [a,b]**	0.33 ± 0.03 (3) [a]*	0.48 ± 0.06 (3) [a]**	0.38 ± 0.05 (3) [b]**	0.0108
Respiratory exchange ratio					
12 h dark	0.97 ± 0.01 (3) [a,b]	0.98 ± 0.01 (3) [a]	0.92 ± 0.02 (3) [b]	0.98 ± 0.03 (3) [a]	0.0205
12 h light	0.90 ± 0.01 (3) [a]**	0.84 ± 0.02 (3) [a,b]**	0.89 ± 0.01 (3) [a]*	0.81 ± 0.03 (3) [b]*	0.0039
Normalized \dot{V}_{O_2} (ml/kg/h)					
12 h dark	3347 ± 170 (3)	3693 ± 170 (3)	3078 ± 472 (3)	3573 ± 251 (3)	0.1507
12 h light	2708 ± 78 (3)**	2424 ± 118 (3)*	2499 ± 385 (3)**	2521 ± 278 (3)**	0.4651
Locomotor activity (beam breaks)					
12 h dark	36895 ± 11833 (3)	47602 ± 11139 (3)	48195 ± 18849 (3)	64500 ± 15020 (3)	0.2178
12 h light	10956 ± 2645 (3)*	16533 ± 7465 (3)*	18110 ± 8102 (3)*	13818 ± 2450 (3)*	0.4894

Means ± SD (sample size); dietary factor: 1-way ANOVA with Bonferroni *post hoc* test ($\alpha \leq 0.05$) [letter]. Cycle factor: one-tailed paired *t*-test.

* $P < 0.05$

** $P < 0.01$

*** $P < 0.001$.

adlib, *ad libitum*; CF, control fed; MHF, moderately high fat diet; pair, isocalorically fed to match CF.

and dark cycles (Fig. 6C and D; 1-way ANOVA with Bonferroni's *post hoc* test). The most interesting of the *post hoc* tests indicated that in females, pair-fed mice had a decreased RER during the dark cycle when consuming MHF (Fig. 6D, right) and an increase in RER when consuming MHF in the light cycle (Fig. 6C, right). In the male mice, *post hoc* tests indicated that MHF-fed mice were significantly different when comparing *ad libitum* vs. pair fed treatments (Fig. 6C and D, left). MHF pair-fed, male mice increased their RER during the dark cycle (Fig. 6D, left) and then decreased it during the light cycle over that of *ad libitum* MHF-fed mice (Fig. 6C, left). Pair feeding or dietary treatment did not affect any other measured metabolic variable in the CLAMS including caloric intake, normalized \dot{V}_{O_2} , normalized \dot{V}_{CO_2} or locomotor activity (non-wheel ambulatory) (Tables 2 and 3), with the exception of body weight, which was previously noted (Figs 4 and 5). The variable of water intake was computed in the CLAMS and reported in Tables 2 and 3; however, it is not as meaningful a measurement because the MHF chow contains water to promote pellet formation and thus mice drink less water when on that

chow. Despite this fact, we did observe that within the CF treatment groups, in females, pair-fed mice drank significantly less in the light cycle, and in males, regardless of light cycle, the pair-fed mice drank significantly more than their CF adlib counterparts (Tables 2 and 3; 1-way ANOVA with Tukey's *post hoc* test). For all the metabolic data, it is well-known that there is a strong difference in all metrics between the light–dark cycle due to mice being nocturnal animals. An analysis across the light–dark cycle within dietary treatment group supported a decrease in all metabolic variables in the light cycle (Tables 2 and 3; one-tailed paired *t*-test, $\alpha = 0.05$).

Voluntary running does not mitigate the loss of OSNs or correlate axonal projections attributed to consumption of fatty diet

If consumption of fat causes a deleterious loss of axonal projections and associated OSNs, we questioned whether an increase in exercise could mitigate this loss. Voluntary exercise, rather than forced, weighted or endurance

Table 3. Metabolic properties in female mice in response to dietary treatment for females

Metabolic property	CF adlib	CF pair	MHF adlib	MHF pair	<i>P</i>
Body weight (g)	24.4 ± 1.3 (3)	22.7 ± 2.3 (3)	28.5 ± 3.6 (4)	23.9 ± 2.3 (3)	0.0619
Water intake (g)					
12 h dark	4.7 ± 1.2 (3) [a,b]	5.7 ± 0.6 (3) [a]	3.7 ± 0.9 (4) [a,b]	2.7 ± 0.3 (3) [b]	0.0089
12 h light	1.7 ± 0.5 (3) [a]*	0.2 ± 0.2 (3) [b]**	1.5 ± 0.2 (4) [a]**	1.6 ± 0.1 (3) [a]**	0.0001
Caloric intake (kcal)					
12 h dark	15.2 ± 4.7 (3)	13.5 ± 3.2 (3)	18.6 ± 2.8 (4)	12.8 ± 0.1 (3)	0.1906
12 h light	9.0 ± 8.2 (3)	0.7 ± 0.1 (3)**	7.7 ± 3.6 (4)**	3.0 ± 1.6 (3)**	0.1380
Energy expenditure (kcal/h)					
12 h dark	0.42 ± 0.04 (3) [a,b]	0.42 ± 0.02 (3) [a]	0.52 ± 0.04 (4) [b]	0.45 ± 0.03 (3)	0.0188
12 h light	0.35 ± 0.03 (3) [a,b]**	0.29 ± 0.03 (3) [a]*	0.43 ± 0.04 (4) [a]**	0.37 ± 0.03 (3) [b]**	0.0023
Respiratory exchange ratio					
12 h dark	0.96 ± 0.01 (3) [a,b]	1.00 ± 0.01 (3) [a]	0.94 ± 0.03 (4) [b]	0.93 ± 0.01 (3) [b]	0.0052
12 h light	0.89 ± 0.01 (3) [a]	0.84 ± 0.02 (3) [b]**	0.88 ± 0.01 (4) [a]*	0.89 ± 0.01 (3) [a]*	0.0011
Normalized \dot{V}_{O_2} (ml/kg/h)					
12 h dark	3587 ± 131 (3)	3690 ± 561 (3)	3663 ± 193 (4)	3774 ± 241 (3)	0.7784
12 h light	3045 ± 135 (3)**	2671 ± 391 (3)*	3129 ± 226 (4)**	3127 ± 277 (3)**	0.2423
Locomotor activity (beam breaks)					
12 h dark	28236 ± 10604 (3)	40276 ± 8586 (3)	29657 ± 2926 (4)	33405 ± 6845 (3)	0.0745
12 h light	13976 ± 4230 (3)*	17241 ± 1853 (3)*	10903 ± 2196 (4)**	11670 ± 7019 (3)**	0.3582

Means ± SD (sample size); dietary factor: 1-way ANOVA with Bonferroni post hoc test ($\alpha \leq 0.05$) [letter]. Cycle factor: one-tailed paired *t*-test.

**P* < 0.05,

***P* < 0.01

****P* < 0.001.

adlib, *ad libitum*; CF, control fed; MHF, moderately-high fat diet; pair, isocalorically fed to match CF.

exercise, is known to further increase EE and lessen general inflammation (Allen *et al.* 2015; Yoshimura *et al.* 2018). M72 τ LacZ male mice that were treated with MHF *ad libitum*, but simultaneously allowed access to voluntary running wheels, did not exhibit a retention of Olfr160 axonal projections (Fig. 7A and B; 1-way ANOVA with Tukey's *post hoc* test). In fact, *post hoc* analyses demonstrated that exercise alone (CF VEx) caused an intermediate loss of axonal projections, which reached statistical significance as shown in Fig. 7C, where the number of Olfr160-expressing OSNs was reduced as a result of exercise only (CF VEx treatment). Body weight remained unchanged in CF mice with access to voluntary running, and in mice treated with MHF diet and access to voluntary running, body weight was intermediate to that of heavier, MHF sedentary mice *vs.* lighter CF mice (Fig. 7D and E; 2-way RM-ANOVA and 1-way ANOVA with Tukey's *post hoc* test, respectively). Similar to that of body weight, the ability to clear glucose and total deposition of adipose tissue was intermediate in mice treated with MHF diet with access to voluntary running compared with that of the MHF sedentary mice *vs.* both

CF mice conditions (Fig. 7F–H; 1-way ANOVA with Tukey's *post hoc* test). Despite the deleterious effects of increased body weight, loss of OSNs, increased adiposity and poorer glucose clearance ability, male mice treated with MHF diet and allowed access to voluntary running engaged in running longer over those maintained on CF diet (Fig. 8). The mice maintained on MHF diet ran approximately twice as many kilometres (CF mice, 5.9 ± 1.7 km *vs.* MHF mice, 11.2 ± 4.7 km; Student's *t*-test), ran at increased velocity (CF mice, 43.1 ± 3.8 rpm *vs.* MHF mice, 63.4 ± 21.4 rpm; Student's *t*-test), and spent more time running in the dark cycle (CF mice, 182.3 ± 48.1 h *vs.* MHF mice, 236.9 ± 25.3 h; Student's *t*-test), compared to that of CF mice.

Discussion

Our combined anatomical and physiological results demonstrate unequivocally that maintaining mice on isocaloric diets induces changes in olfactory circuitry that are dependent upon food content and now cannot be solely

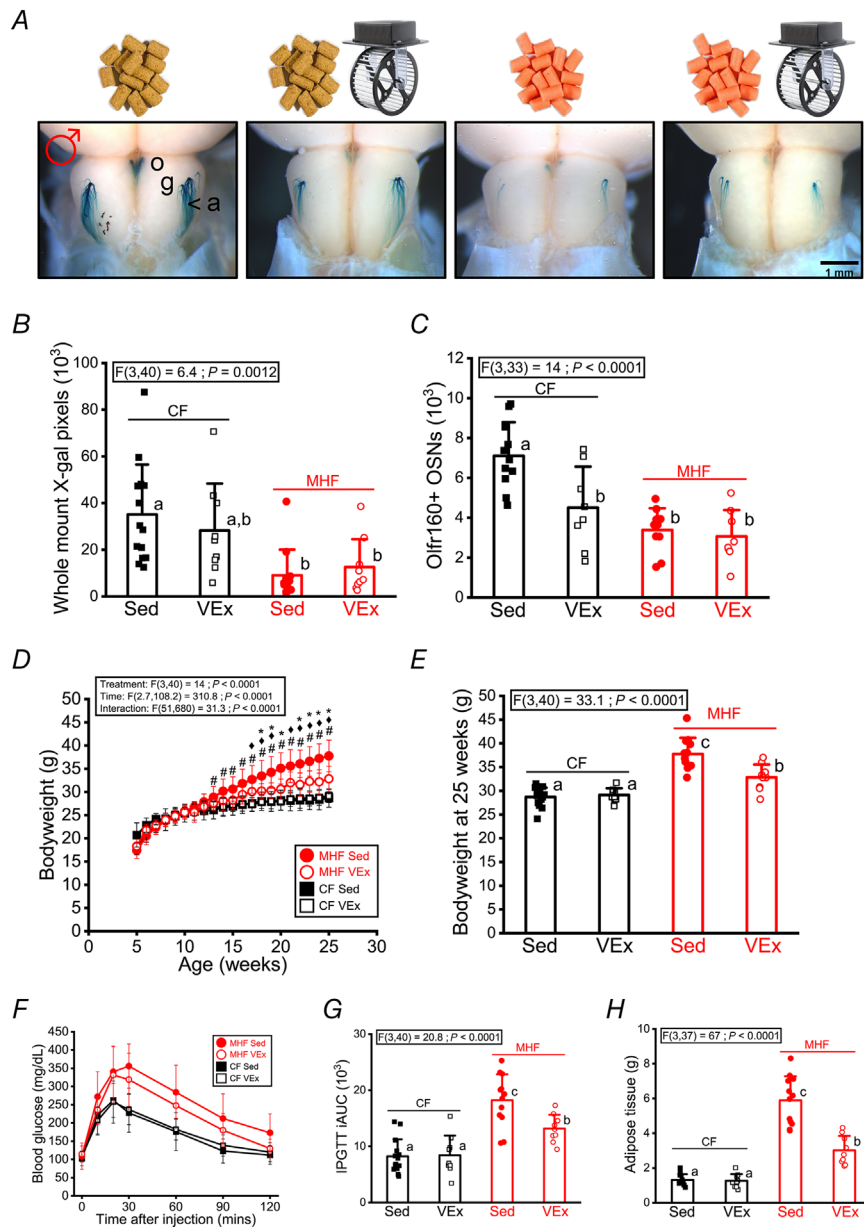


Figure 7. Voluntary running does not mitigate the loss of Olf160-axonal projections and Olf160-expressing OSNs elicited by consumption of a fatty diet

A, representative whole-mount images of olfactory bulbs following β -galactosidase histological staining of Olf160-expressing olfactory sensory neurons (OSNs) from male M72*tau*LacZ mice following diet/exercise treatments. Images from left to right: control diet *ad libitum* (brown food symbol), control diet plus running wheel (brown food and wheel symbol), moderately high-fat diet *ad libitum* (pink food symbol), moderately high-fat diet plus running wheel (pink food and wheel symbol). Projections were converted to pixel density and OSNs manually counted as in Figs 2 and 3. o, olfactory bulb; g, glomerulus; a, Olf160 axonal projections. **B** and **C**, bar graphs of pixel density of axonal projections (**B**) and number of Olf160-expressing OSNs vs. diet/exercise treatment (**C**). CF Sed, control diet sedentary; CF VEx, control diet voluntary exercise; MHF, moderately high-fat diet sedentary; MHF VEx, moderately high-fat diet voluntary exercise. **D**, line graph of body weight vs. age; 2-way RM-ANOVA. Symbols indicate significantly different for treatment factor as determined by Tukey's *post hoc* ($P < 0.05$) as follows: #, MHF Sed > both CF groups; \diamond , MHF VEx > both CF groups; *, MHF Sed > MHF VEx. **E**, bar graph of body weight vs. diet/exercise treatment at 25 weeks of age. **F** and **G**, line graph of the plasma glucose concentration (**F**) and bar graph of the iAUC during the IPGTT (**G**). **H**, bar graph of the total excised adipose tissue vs. diet/exercise treatment. Notations as in Fig. 2. **B**, **C**, **E**, **G**, **H**, 1-way ANOVA, Tukey's *post hoc*, $P < 0.05$. Sample sizes in number of mice from left to right for whole mount: 14, 9, 12, 9; for neuronal counts: 11, 8, 10, 8; for body weight and IPGTT: 14, 9, 12, 9; and for adipose tissue: 11, 9, 12, 9.

attributed to an obesogenic diet. In a sex-independent manner, mice that consumed a MHF chow exhibited a loss of OSNs and axonal projections to defined synaptic targets, independent of whether this consumption induced adiposity and body weight gain. Moreover, increased EE through access to voluntary running failed to mitigate the loss of the neurons and associated circuitry.

A comparison of the maintenance of OSNs in male vs. female mice challenged with different nutritional environments has not been reported previously to our knowledge. Mouse strains are differentially sensitive to obesogenic diets and thus the variables of sex and age are important when selecting an appropriate model (Nishikawa *et al.* 2007). The fact that female C57BL6/J mice strains are resistant to DIO (Yang *et al.* 2014) provided us with a secondary opportunity to test whether adiposity was necessary to induce a loss of OSNs. Both female mice and pair fed male mice failed to gain significant adipose deposits or fat tissue mass while consuming MHF diets over 5 months, yet still exhibited loss of OSNs and associated axonal projections. It is well known that an imbalance in energy homeostasis causes the development of a higher fat mass, which is associated with a low-grade inflammation (Xu *et al.* 2003a; Saltiel & Olefsky, 2017; Xu *et al.* 2021). Low grade inflammation has been reported frequently in conjunction with obese mouse models (Gregor & Hotamisligil, 2011; Kaufman *et al.* 2018; Duffy *et al.* 2019). Moreover, adipocyte-derived chemokines, such as TNF α , are associated with precipitation of insulin resistance, reduced glucose clearance and prediabetes (Hotamisligil *et al.* 1993; Xu *et al.* 2003a, 2015; Bodzin & Saltiel, 2007; Wensveen *et al.* 2015). Although we did not observe a significant elevation in interleukins that has been observed with the induction of obesity (Emerson *et al.* 2017), TNF α was elevated in a sex-independent manner in both *ad libitum* and pair-fed treatments, inferring the activation of chemokines with consumption of a fatty diet, and not just

attributable to adiposity *per se*. This is consistent with our sex-independent finding of the disruption in glucose clearance in both *ad libitum* and pair-fed treatments. It is highly interesting to note that DIO-resistant females retain an inability to clear glucose, an index of reduced metabolic health, despite lack of adipocyte accumulation. Because TNF α mediates apoptotic cell death (Idriss & Naismith, 2000) and its induced expression in the olfactory epithelium results in a significant loss of OSNs (Sultan *et al.* 2011; Sousa Garcia *et al.* 2017; Torabi *et al.* 2020), our measured elevation of this cytokine following both MHF treatments is consistent with the observed concomitant loss of OSNs. It is also conceivable, seeing as adipose tissue is not the only source of inflammation, that our observed increased TNF α is the result of an inflammatory pathway partially or entirely unrelated to adipocytes. In fact, other groups have observed increased TNF α in high fat feeding independent of obesity. For example, Delahaye *et al.* (2018) used a time-restricted feeding intervention with a 45% fat diet that reduced weight gain and body fat but not circulating TNF α (Delahaye *et al.* 2018).

Our study used the M72*tauLacZ* mouse line as a tractable model due to its ability to identify a specific genetic reporter for a single odorant receptor (*Olf160*). The results of our study might be restricted to only a subtype of ORs, albeit the design being a helpful tool to visualize the effects of a fat diet on the structure of the olfactory system. Because the mouse olfactory gene family is estimated to have 1000 ORs, we cannot definitively conclude that fat in the diet results in significant loss of all classes of OSNs. In previous work from our laboratory, however, we have demonstrated that DIO causes loss of G α_{olf} protein and MOR28 (*Olf1507*), as well as a reduction in olfactory marker protein positive neurons (mature OSNs) (Thiebaud *et al.* 2014). These parallel data suggest that it is not unlikely that the results of our current study extend beyond effects on M72-expressing OSNs.

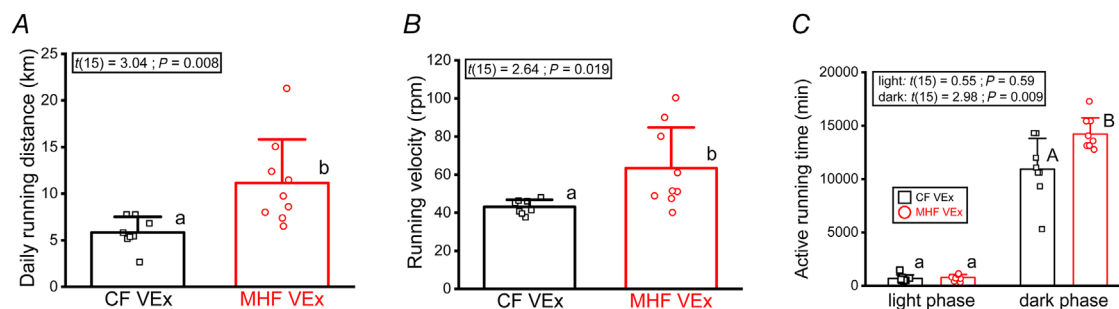


Figure 8. Mice spend more time running for greater distances and with increased velocity when provided a fatty diet

Bar graph of the mean daily running distance (A), velocity (B), and duration (C) in M72*tauLacZ* male mice sampled from a 28-day continuous interval within the 6-month experimental exercise block. Abbreviations and statistical notations as in Fig. 6; analysed by Student's *t*-test for mean 24 h (A and B) or 12 h (C) time blocks. Sample sizes in number of mice: CF VEX: 8; MHF VEX: 9.

Because isocaloric consumption of MHF diet without associated adiposity caused loss of OSNs, we wondered whether consumption of fat might also cause a reduction in odour detection or ability to detect odours. While our pair-fed data do not directly address olfactory ability, we and others have demonstrated that induction of DIO causes a loss in EOG amplitude (Thiebaud *et al.* 2014; Lacroix *et al.* 2015; Riviere *et al.* 2016) signifying reduced olfactory sensitivity. Odour-evoked EOG amplitude is proportional to the number of OSNs whereas the decay time is an indication of odour adaptation. Mice maintained on excess nutrition exhibit not only loss in olfactory structures, but loss in G-protein-coupled machinery, reductions in odour receptors, and poorer odour discrimination using habituation/dishabituation trials, conditioned-odour aversion or go–no-go operant conditioning paradigms (Fadool *et al.* 2011; Tucker *et al.* 2012a; Aimé *et al.* 2014; Thiebaud *et al.* 2014; Lacroix *et al.* 2015; Fardone *et al.* 2018). One might therefore conjecture that the loss of OSNs in isocalorically, MHF-treated mice would lead to a loss in EOG amplitude and reduced olfactory ability; however, the type of nutrition may be an important variable. A good example is the study of Riviere *et al.* (2016) who generated DIO in mice using 60% fructose rather than high fat, and discovered reduced EOG amplitude and reduced odour discrimination, but curiously, an increase in OMP⁺ mature OSNs (Riviere *et al.* 2016). Rather than losing OSNs with poor nutrition, the mice in their experiments exhibited reduced apoptosis following the fructose supplementation. While a reduced EOG amplitude seems counterintuitive to an increase in OSNs, the authors hypothesize that the OMP⁺ mature neurons are ageing neurons with reduced transduction properties. Therefore, a change in diet caused a change in OSN cell dynamics (newborn, mature, *vs.* ageing), which is very interesting. Clearly future experiments should test whether pair feeding regimens cause a behavioural or electrical change in olfactory ability concurrent with a loss in olfactory structures or change in cell turnover.

In terms of metabolism, our data demonstrate changes in EE and fuel utilization (RER) associated with dietary treatment in both male and female mice. The enhanced EE we measured in MHF *ad libitum*-treated mice would be consistent with a higher fat mass in mice following DIO. However, it is curious that increased adiposity was only observed in male mice and the increased EE was also observed in the female mice that were relatively resistant to obesity. Interestingly, utilization of fuel (RER) in MHF-treated male mice was significantly different across the *ad libitum vs.* pair-fed treatments. Considering that loss of olfactory structures (axonal projections and OSNs) was congruent between these two conditions, this suggests that olfactory loss is not necessarily always correlated to changes in predominant fuel utilization.

When MHF was pair fed, male mice increased the use of carbohydrates for fuel during the dark cycle (RER increased) and relied more on fats during the light cycle (RER decreased), whereas MHF *ad libitum*-treated mice had a stable RER regardless of light cycle. While our interpretation cannot directly include olfactory ability (we cannot assume loss of OSNs = loss of olfactory ability), we and others have previously shown a relationship between metabolism and olfactory ability (Fadool *et al.* 2004; Riera *et al.* 2017). Kv1.3^{-/-} mice are notably super-smellers in terms of olfactory discrimination and threshold, are thin and are resistant to DIO (Xu *et al.* 2003b, 2004; Upadhyay *et al.* 2013; Thiebaud *et al.* 2014; Riera *et al.* 2017), and blocking Kv1.3 in the olfactory bulb causes a reduction in RER in the light cycle (Schwartz *et al.* 2021). Mice with loss of olfactory ability due to genetic ablation of OSNs were found to have an increase in EE and be resistant to DIO (Riera *et al.* 2017). Pair feeding appears to uncouple these types of metabolic relationships in that loss of OSNs is retained but use of fuels and EE are uncorrelated.

Our data demonstrated that running itself can cause loss of OSNs independent of diet because mice maintained on purely CF diets and allowed access to running wheels had fewer OSNs than sedentary mice. Poor health factors such as reduced glucose clearance or increased adiposity were not observed for mice on CF diets, despite the loss of OSNs, suggesting that other factors can contribute to OSN loss that relate to exercise alone. Certainly, exercise inherently increases EE (Alghannam *et al.* 2021), but we have demonstrated that EE that becomes uncoupled during isocaloric feeding is not correlated to OSN abundance. It is known that different inflammatory signalling pathways are reduced depending upon the type and duration of exercise (Hicks *et al.* 2016; Yoshimura *et al.* 2018; Scheffer & Latina, 2020). Inflammation that is reduced with voluntary running may not be sufficient to maintain olfactory neuronal circuits and OSNs in response to a long-term consumption of a hyperlipidaemic diet. While general ambulatory locomotor activity (non-wheel based) was not impacted by fat- or pair-feeding (Tables 2 and 3), running activity itself was significantly enhanced by increased available calories. And while running did improve health metrics of glucose clearance and adiposity in the MHF-treated mice, this was not able to rescue OSN abundance or neuronal circuits.

Exercise regimens have long been prescribed to patients suffering from DIO in an attempt to reduce chronic systemic inflammation (Scheffer & Latina, 2020). It was therefore very unexpected that voluntary exercise was not protective against the obesity-induced loss of OSNs. Other studies investigating the protective potential of exercise have seen certain neuroprotective benefits from treadmill exercise and swimming (Li *et al.* 2017; Lu *et al.* 2017; Lourenco *et al.* 2019). It is possible that the mice

in our study were not running enough voluntarily to produce these effects. It will be important to investigate other types of exercise outside of that which is entirely voluntary considering the propensity of high-fat diets to reduce spontaneous physical activity (Bjursell *et al.* 2008; Levine *et al.* 2008; Schmidt *et al.* 2012; Friend *et al.* 2017). Additionally, we know from Borg *et al.* (2012) that subjecting high fat diet-fed mice to endurance exercise training was not able to prevent an accumulation of lipids in the hypothalamus (Borg *et al.* 2012). If we surmise that neurodegeneration in olfactory structures is partially brought on by lipotoxicity, it might be logical that voluntary exercise is unable to rescue OSN abundance or associated neuronal projections.

In designing our study, we discovered that little is known about how exercise impacts the olfactory system. In trained detection dogs, a 30-min forced treadmill exercise session reduced the ability to locate a target odour (Angle *et al.* 2014). In humans, exercise improved inspiratory flow through the nose, but this did not result in improved olfactory detection (Marioni *et al.* 2010). A 10-year longitudinal study and a separate 1-year study in aged humans revealed that exercise decreased the risk of developing an olfactory impairment (Schubert *et al.* 2013; Zhang *et al.* 2020). Results from other studies investigating the effect of exercise specifically on olfactory neurons are scarce and mixed. Brown *et al.* (2003) showed that voluntary wheel running for ~40 days did not increase neurogenesis in the OB as measured by bromodeoxyuridine (BrdU) labelling of granule cells (Brown *et al.* 2003). More recent studies, however, have demonstrated increased neurogenesis in the subventricular zone. One group used treadmill running in a mouse model of depression generated via chronic unpredictable mild stress, preventing dopaminergic neuron loss in the glomerular layer and improving olfactory function (Tian *et al.* 2020). Other studies have observed rescue effects of wheel running on neural stem cells that were made defective by genetic manipulation or chronic corticosterone infusion (Brown *et al.* 2003; Mastroianni *et al.* 2017). Chae *et al.* (2014) observed increased BrdU labelling and increased doublecortin (a marker for neuronal progenitors) in the subventricular zone of rats following 8 weeks of swimming exercise (Chae *et al.* 2014). Conversely in the OE, another group reported decreased mature OSNs (OMP-positive) and increased apoptotic OSNs following wheel running exercise in mice that they attributed to oxidative stress (Tuerdi *et al.* 2018). It is important to note that different exercise modalities can have different effects on a given parameter. For example, forced exercise and voluntary exercise have been shown to have opposing effects on microbiota, and moderate intensity exercise decreases inflammatory cytokines, whereas high-intensity exercise increases them (Allen *et al.* 2015; Paolucci *et al.*

2018). In the olfactory system, however, different research groups observed different outcomes despite similar wheel running treatments.

Given the lack of olfactory neuroprotection against DIO afforded by voluntary exercise, it will be important to investigate ways in which other diets or dietary compositions can influence sensory neuron development. Future experiments should determine the duration or critical period for exposure to dietary fat as well as recognize other mechanisms beyond inflammation for which dietary fat might trigger poor health. For example, ketogenic diets have been reported to benefit individuals suffering from epilepsy, cancer, neuronal loss and cognitive deficits (Newman *et al.* 2017; Roberts *et al.* 2017; Li *et al.* 2020), but their high-fat nature may be disruptive to sensory neurons and hence satiety signals. It is important to recognize that the full macronutrient breakdown of the two diets in our study is as follows: MHF: 32% fat, 51% carbohydrate and 17% protein; CF: 13.5% fat, 58% carbohydrate and 28.5% protein. Therefore, an alternative interpretation is that the MHF diet could be a low protein diet and not only a MHF diet. Low protein diets have been shown to slow down cancer progression, increase longevity and mitigate kidney disease (Roberts *et al.* 2017; Rhee *et al.* 2018; Rubio-Patino *et al.* 2018). It seems unlikely that the lower protein content could trigger inflammation or lead to neuronal loss in the olfactory system, but it is a possibility that should be explored. Also, the CF and MHF diets contain approximately the same amounts of saturated fat *vs.* unsaturated, but the unsaturated fat sources are notably different. The MHF diet contains much higher levels of ω -6 fatty acids, which are associated with low-grade inflammation, and lower amounts of the ω -3 fatty acids, which have been demonstrated to be anti-inflammatory (Delpech *et al.* 2015; Layé *et al.* 2018). Finally, the duration of dietary challenge is a variable that should be explored. Monteni *et al.* (2002) discovered both a reduction in hippocampal plasticity and a reduced performance on the Morris water maze (a standard test for spatial learning and memory) following only 2 months on a high-fat, refined-sugar diet (Monteni *et al.* 2002). Another group observed impaired memory and increased anxiety-like behaviours in mice following only 1 week on a high-fat diet (Kaczmarczyk *et al.* 2013). It is possible that the neuronal loss observed in the olfactory system occurs much sooner than the termination points used in our pair-feeding experiments and in Thiebaud *et al.* (2014). Finally, fat in the diet can have deleterious effects outside of adipocyte-linked inflammation that can be investigated for effects on OSN development. For example, high-fat diets increase intestinal permeability, which leads to increased levels of circulating lipopolysaccharide (a component of Gram-negative bacteria that live in the gut; an inflammatory endotoxin) (Moreira *et al.* 2012). Fatty

diets can also increase the levels of circulating free fatty acids, which have been shown to induce inflammation through toll-like receptors (Eguchi & Nagai, 2017).

To recapitulate, our study demonstrates that a long-term macronutrient imbalance in dietary fat can cause a loss of OSNs and associated bulbar connections. Maintenance of MHF pair feeding in mice does not elicit increased deposition of adipose tissue but changes cytokine production and the animal's ability to clear glucose, rendering the mouse in a less physiologically healthy state. Increased EE through voluntary running does not mitigate the deleterious effects of the fatty diet – mice still show a loss of OSNs and bulbar projections. Patterns of long-term dietary consumption may play a distinct role in olfactory discrimination and food choice attributed to reshaping neuronal abundance and communication in the olfactory system.

References

- Aimé P, Palouzier-Paulignan B, Salem R, Al Koborssy D, Garcia S, Duchamp C, Romestaing C & Julliard AK (2014). Modulation of olfactory sensitivity and glucose-sensing by the feeding state in obese Zucker rats. *Front Behav Neurosci* **8**, 326.
- Alghannam AF, Ghaith MM & Alhussain MH (2021). Regulation of energy substrate metabolism in endurance exercise. *Int J Env Res Pub Heal* **18**, 4963.
- Allen JM, Berg Miller ME, Pence BD, Whitlock K, Nehra V, Gaskins HR, White BA, Fryer JD & Woods JA (2015). Voluntary and forced exercise differentially alters the gut microbiome in C57BL/6J mice. *J Appl Physiol* **118**, 1059–1066.
- Angle CT, Wakshlag JJ, Gillette RL, Steury T, Haney P, Barrett J & Fisher T (2014). The effects of exercise and diet on olfactory capability in detection dogs. *J Nutr Sci* **3**, e44.
- Biju KC, Marks DR, Mast TG & Fadool DA (2008). Deletion of voltage-gated channel affects glomerular refinement and odorant receptor expression in the mouse olfactory system. *J Comp Neurol* **506**, 161–179.
- Bjursell M, Gerdin AK, Lelliott CJ, Egecioglu E, Elmgren A, Tornell J, Oscarsson J & Bohlooly YM (2008). Acutely reduced locomotor activity is a major contributor to Western diet-induced obesity in mice. *Am J Physiol Endocrinol Metab* **294**, E251–E260.
- Bodzin CN & Saltiel AR (2007). Obesity induces a phenotypic switch in adipose tissue macrophage polarization. *J Clin Invest* **117**, 175–184.
- Borg ML, Omran SF, Weir J, Meikle PJ & Watt MJ (2012). Consumption of a high-fat diet, but not regular endurance exercise training, regulates hypothalamic lipid accumulation in mice. *J Physiol* **590**, 4377–4389.
- Brown J, Cooper-Kuhn CM, Kempermann G, Van Praag H, Winkler J, Gage FH & Kuhn HG (2003). Enriched environment and physical activity stimulate hippocampal but not olfactory bulb neurogenesis. *Eur J Neurosci* **17**, 2042–2046.
- Chae CH, Jung SL, An SH, Park BY, Kim TW, Wang SW, Kim JH, Lee HC & Kim HT (2014). Swimming exercise stimulates neurogenesis in the subventricular zone via increase in synapsin I and nerve growth factor levels. *Biol Sport* **31**, 309–314.
- Chelette BM, Thomas AM & Fadool DA (2019). Long-term obesogenic diet and targeted deletion of potassium channel $K_v1.3$ have differing effects on voluntary exercise in mice. *Physiol Rep* **7**, e14254.
- Delahaye LB, Bloomer RJ, Butawan MB, Wyman JM, Lee HW, Liu AC, McAllan L, Han JC & van der Merwe M (2018). Time-restricted feeding of a high-fat diet in male C57BL/6 mice reduces adiposity but does not protect against increased systemic inflammation. *Appl Physiol Nutr Metab* **43**, 1033–1042.
- Delpech JC, Madore C, Joffre C, Aubert A, Kang JX, Nadjar A & Laye S (2015). Transgenic increase in n-3/n-6 fatty acid ratio protects against cognitive deficits induced by an immune challenge through decrease of neuroinflammation. *Neuropsychopharmacology* **40**, 525–536.
- Duffy CM, Hofmeister JJ, Nixon JP & Butterick TA (2019). High fat diet increases cognitive decline and neuroinflammation in a model of orexin loss. *Neurobiol Learn Mem* **157**, 41.
- Eguchi K & Nagai R (2017). Islet inflammation in type 2 diabetes and physiology. *J Clin Invest* **127**, 14–23.
- Emerson SR, Kurti SP, Harms CA, Haub MD, Melgarejo T, Logan C & Rosenkranz SK (2017). Magnitude and timing of the postprandial inflammatory response to a high-fat meal in healthy adults: a systematic review. *Adv Nutr* **8**, 213–225.
- Fadool DA, Tucker K & Pedarzani P (2011). Mitral cells of the olfactory bulb perform metabolic sensing and are disrupted by obesity at the level of the $K_v1.3$ ion channel. *PLoS One* **6**, e24921.
- Fadool DA, Tucker K, Perkins R, Fasciani G, Thompson RN, Parsons AD, Overton JM, Koni PA, Flavell RA & Kaczmarek LK (2004). $K_v1.3$ channel gene-targeted deletion produces “super-smeller mice” with altered glomeruli, interacting scaffolding proteins, and biophysics. *Neuron* **41**, 389–404.
- Fardone E, Celen AB, Schreiter NA, Thiebaud N, Cooper ML & Fadool DA (2018). Loss of odor-induced c-Fos expression of juxtglomerular activity following maintenance of mice on fatty diets. *J Bioenerg Biomembr* **51**, 3–13.
- Friend DM, Devarakonda K, O'Neal TJ, Skirzewski M, Papazoglou I, Kaplan AR, Liow JS, Guo J, Rane SG, Rubinstein M, Alvarez VA, Hall KD & Kravitz A V (2017). Basal ganglia dysfunction contributes to physical inactivity in obesity. *Cell Metab* **25**, 312–321.
- Gregor MF & Hotamisligil GS (2011). Inflammatory mechanisms in obesity. *Annu Rev Immunol* **29**, 415.
- Grundy D (2015). Principles and standards for reporting animal experiments in *The Journal of Physiology* and *Experimental Physiology*. *J Physiol* **593**, 2547–2549.
- Hicks JA, Hatzidis A, Arruda NL, Gelineau RR, De Pina IM, Adams KW & Seggio JA (2016). Voluntary wheel-running attenuates insulin and weight gain and affects anxiety-like behaviors in C57BL6/J mice exposed to a high-fat diet. *Behav Brain Res* **310**, 1–10.

- Hotamisligil G (2006). Inflammation and metabolic disorders. *Nature* **444**, 860–867.
- Hotamisligil GS, Shargill NS & Spiegelman BM (1993). Adipose expression of tumor necrosis factor- α : direct role in obesity-linked insulin resistance. *Science* **259**, 87–91.
- Idriss HT & Naismith JH (2000). TNF α and the TNF receptor superfamily: structure-function relationship(s). *Microsc Res Tech* **50**, 184–195.
- Kaczmarczyk MM, Machaj AS, Chiu GS, Lawson MA, Gainey SJ, York JM, Meling DD, Martin SA, Kwakwa KA, Newman AF, Woods JA, Kelley KW, Wang Y, Miller MJ & Freund GG (2013). Methylphenidate prevents high-fat diet (HFD)-induced learning/memory impairment in juvenile mice. *Psychoneuroendocrinology* **38**, 1553–1564.
- Kaufman A, Choo E, Koh A & Dando R (2018). Inflammation arising from obesity reduces taste bud abundance and inhibits renewal. *PLoS Biol* **16**, e2001959.
- Kolling LJ & Fadool DA (2020). Role of olfaction for eating behavior. In *The Senses: A Comprehensive Reference*, ed. Fritsch B & Meyerhof W, pp. 675–716. Elsevier, Academic Press.
- Kovach CP, Al KD, Huang Z, Chelette BM, Fadool JM & Fadool DA (2016). Mitochondrial ultrastructure and glucose signaling pathways attributed to the Kv1.3 ion channel. *Front Physiol* **7**, 178.
- Lacroix MC, Caillol M, Durieux D, Monnerie R, Grebert D, Pellerin L, Repond C, Tolle V, Zizzari P & Baly C (2015). Long-lasting metabolic imbalance related to obesity alters olfactory tissue homeostasis and impairs olfactory-driven behaviors. *Chem Senses* **40**, 537–556.
- Layé S, Nadjar A, Joffre C & Bazinet RP (2018). Anti-inflammatory effects of omega-3 fatty acids in the brain: physiological mechanisms and relevance to pharmacology. *Pharm Rev* **70**, 12–38.
- Levine JA, McCrady SK, Lanningham-Foster LM, Kane PH, Foster RC & Manohar CU (2008). The role of free-living daily walking in human weight gain and obesity. *Diabetes* **57**, 548–554.
- Li DJ, Li YH, Yuan HB, Qu LF & Wang P (2017). The novel exercise-induced hormone irisin protects against neuronal injury via activation of the Akt and ERK1/2 signaling pathways and contributes to the neuroprotection of physical exercise in cerebral ischemia. *Metab Clin Exp* **68**, 31.
- Li RJ, Liu Y, Liu HQ & Li J (2020). Ketogenic diets and protective mechanisms in epilepsy, metabolic disorders, cancer, neuronal loss, and muscle and nerve degeneration. *J Food Biochem* **44**, e13140.
- Lourenco MV, Frozza RL, de Freitas GB, Zhang H, Kincheski GC, Ribeiro FC, Gonçalves RA, Clarke JR, Beckman D, Staniszewski A, Berman H, Guerra LA, Forny-Germano L, Meier S, Wilcock DM, de Souza JM, Alves-Leon S, Prado VF, Prado MAM, Abisambra JF, Tovar-Moll F, Mattos P, Arancio O, Ferreira ST & De Felice FG (2019). Exercise-linked FNDC5/irisin rescues synaptic plasticity and memory defects in Alzheimer's models. *Nat Med* **25**, 165–175.
- Lu Y, Dong Y, Tucker D, Wang R, Ahmed ME, Brann D & Zhang Q (2017). Treadmill exercise exerts neuroprotection and regulates microglial polarization and oxidative stress in a streptozotocin-induced rat model of sporadic Alzheimer's disease. *J Alzh Dis* **56**, 1469–1484.
- Lusk G & Du Bois EF (1924). On the constancy of the basal metabolism. *J Physiol* **59**, 213–216.
- Marioni G, Ottaviano G, Staffieri A, Zaccaria M, Lund VJ, Tognazza E, Coles S, Pavan P, Brugin E & Ermalao A (2010). Nasal functional modifications after physical exercise: olfactory threshold and peak nasal inspiratory flow. *Rhinology* **48**, 277–280.
- Mastrorilli V, Scopa C, Saraulli D, Costanzi M, Scardigli R, Rouault JP, Farioli-Vecchioli S & Tirone F (2017). Physical exercise rescues defective neural stem cells and neurogenesis in the adult subventricular zone of Btg1 knockout mice. *Brain Struct Funct* **222**, 2855–2876.
- Monteni R, Barnard RJ, Ying Z, Roberts CK & Gomez-Pinilla F (2002). A high-fat, refined sugar diet reduces hippocampal brain-derived neurotrophic factor, neuronal plasticity, and learning. *Neuroscience* **112**, 803–814.
- Moreira AP, Texeira TF, Ferreira AB, Peluzio Mdo C & de Cássia Gonçalves Alfenas R (2012). Influence of a high-fat diet on gut microbiota, intestinal permeability and metabolic endotoxaemia. *Br J Nutr* **108**, 801–809.
- Newman JC, Covarrubias AJ, Zhao M, Yu X, Gut P, Ng CP, Huang Y, Haldar S & Verdin E (2017). Ketogenic diet reduces midlife mortality and improves memory in aging mice. *Cell Metab* **26**, 547–557.e8.
- Nishikawa S, Yasoshima A, Doi K, Nakayama H & Uetsuka K (2007). Involvement of sex, strain and age factors in high fat diet-induced obesity in C57BL/6J and BALB/cA mice. *Exp Anim* **56**, 263–272.
- Palouzier-Paulignan B, Lacroix M, Aimé P, Baly C, Caillol M, Congar P, Julliard A, Tucker K & Fadool D (2012). Olfaction under metabolic influences. *Chem Senses* **37**, 769–797.
- Paolucci EM, Loukov D, Bowdish D & Heisz JJ (2018). Exercise reduces depression and inflammation but intensity matters. *Biol Psychol* **133**, 79.
- Rhee CM, Ahmadi SF, Kovesdy CP & Kalantar-Zadeh K (2018). Low-protein diet for conservative management of chronic kidney disease: a systematic review and meta-analysis of controlled trials. *J Cach Sarco Mus* **9**, 235–245.
- Riera CE, Tsousidou E, Halloran J, Follett P, Hahn O, Pereira MMA, Ruud LE, Alber J, Tharp K, Anderson CM, Bronneke H, Hampel B, Filho CDM, Stahl A, Bruning JC & Dillin A (2017). The sense of smell impacts metabolic health and obesity. *Cell Metab* **26**, 198–211.e5.
- Riviere S, Soubeyre V, Jarriault D, Molinas A, Leger-Charnay E, Desmoulin L, Grebert D, Meunier N & Grosmaître X (2016). High fructose diet inducing diabetes rapidly impacts olfactory epithelium and behavior in mice. *Sci Rep* **6**, 34011.
- Roberts MN, Wallace MA, Tomilov AA, Zhou Z, Marcotte GR, Tran D, Perez G, Gutierrez-Casado E, Koike S, Knotts TA, Imai DM, Griffey SM, Kim K, Hagopian K, Haj FG, Baar K, Cortopassi GA, Ramsey JJ & Lopez-Dominguez JA (2017). A ketogenic diet extends longevity and healthspan in adult mice. *Cell Metab* **26**, 539–546.e5.

- Rubio-Patino C, Bossowski JP, De Donatis GM, Mondragón L, Villa E, Aira LE, Chiche J, Mhaidly R, Lebeaupein C, Marchetti S, Voutetakis K, Chatziioannou A, Castelli FA, Lamourette P, Chu-Van E, Fenaille F, Avril T, Passeron T, Patterson JB, Verhoeven E, Bailly-Maitre B, Chevet E & Ricci JE (2018). Low-protein diet induces IRE1 α dependent anticancer immunosurveillance. *Cell Metab* **27**, 828–842.
- Saltiel AR & Olefsky JM (2017). Inflammatory mechanisms linking obesity and metabolic disease. *J Clin Invest* **127**, 1–4.
- Scheffer D & Latina A (2020). Exercise-induced immune system response: anti-inflammatory status on peripheral and central organs. *Biochim Biophys Acta* **1866**, 165823.
- Schindelin J, Arganda-Carreras I & Frise E (2012). Fiji: An open-source platform for biological-image analysis. *Nat Methods* **9**, 676–682.
- Schmidt SL, Harmon KA, Sharp TA, Kealey EH & Bessesen DH (2012). The effects of overfeeding on spontaneous physical activity in obesity prone and obesity resistant humans. *Obesity* **20**, 2186–2193.
- Schubert CR, Cruickshanks KJ, Nondahl DM, Klein BE, Klein R & Fischer ME (2013). Association of exercise with lower long-term risk of olfactory impairment in older adults. *JAMA Otolaryngol Head Neck Surg* **139**, 1061–1066.
- Schwartz AB, Kapur A, Huang Z, Anangi R, Spear JM, Staggs S, Fardone E, Dekan Z, Rosenberg JT, Grant SC, King GF, Mattoussi H & Fadool DA (2021). Olfactory bulb-targeted quantum dot (QD) bioconjugate and Kv1.3 blocking peptide improve metabolic health in obese male mice. *J Neurochem* **157**, 1876–1896.
- Scott J & Scott-Johnson P (2002). The electroolfactogram: a review of its history and uses. *Microsc Res Tech* **58**, 152–160.
- Sousa Garcia D, Chen M, Smith AK, Lazarini PR & Lane AP (2017). Role of the type I tumor necrosis factor receptor in inflammation-associated olfactory dysfunction. *Intern Forum Allergy Rhino* **7**, 160–168.
- Sultan B, May LA & Lane AP (2011). The role of TNF- α in inflammatory olfactory loss. *Laryngoscope* **121**, 2481–2486.
- Thiebaud N, Johnson MC, Butler JL, Bell GA, Ferguson KL, Fadool AR, Fadool JC, Gale AM, Gale DS & Fadool DA (2014). Hyperlipidemic diet causes loss of olfactory sensory neurons, reduces olfactory discrimination, and disrupts odor-reversal learning. *J Neurosci* **34**, 6970–6984.
- Tian Y, Dong J & Shi D (2020). Protection of DAergic neurons mediates treadmill running attenuated olfactory deficits and olfactory neurogenesis promotion in depression model. *Biochem Biophys Res Commun* **521**, 725–731.
- Torabi A, Mohammadbagheri E, Akbari Dilmaghani N, Bayat AH, Fathi M, Vakili K, Alizadeh R, Rezaeimirghaed O, Hajiesmaeili M, Ramezani M, Simani L & Aliaghaei A (2020). Proinflammatory cytokines in the olfactory mucosa result in COVID-19 induced anosmia. *ACS Chem Neurosci* **11**, 1909–1913.
- Tucker K, Overton JM & Fadool DA (2008). Kv1.3 gene-targeted deletion alters longevity and reduces adiposity by increasing locomotion and metabolism in melanocortin-4 receptor-null mice. *Int J Obes* **32**, 1222–1232.
- Tucker K, Overton JM & Fadool DA (2012a). Diet-induced obesity resistance of Kv1.3 $^{-/-}$ mice is olfactory bulb dependent. *J Neuroendocr* **24**, 1087–1095.
- Tucker KR, Godbey SJ, Thiebaud N & Fadool DA (2012b). Olfactory ability and object memory in three mouse models of varying body weight, metabolic hormones, and adiposity. *Physiol Behav* **107**, 424–432.
- Tuerdi A, Kikuta S, Kinoshita M, Kamogashira T, Kondo K, Iwasaki S & Yamasoba T (2018). Dorsal-zone-specific reduction of sensory neuron density in the olfactory epithelium following long-term exercise or caloric restriction. *Sci Rep* **8**, 17300.
- Upadhyay SK, Eckel-Mahan KL, Mirbolooki MR, Tjong I, Griffey SM, Schmunk G, Koehne A, Halbout B, Iadonato S, Pedersen B, Borrelli E, Wang PH, Mukherjee J, Sassone-Corsi P & Chandy KG (2013). Selective Kv1.3 channel blocker as therapeutic for obesity and insulin resistance. *Proc Natl Acad Sci U S A* **110**, E2239–E2248.
- Wensveen FM, Valentic S, Sestan M, Turk Wensveen T & Polic B (2015). The “Big Bang” in obese fat: events initiating obesity-induced adipose tissue inflammation. *Eur J Immunol* **45**, 2446–2456.
- Xu H, Barnes GT, Yang Q, Tan G, Yang D, Chou CJ, Sole J, Nichols A, Ross JS, Tartaglia LA & Chen H (2003a). Chronic inflammation in fat plays a crucial role in the development of obesity-related insulin resistance. *J Clin Invest* **112**, 1821–1830.
- Xu J, Koni PA, Wang P, Li G, Kaczmarek LK, Wu Y, Li Y, Flavell RA & Desir GV (2003b). The voltage-gated potassium channel Kv1.3 regulates energy homeostasis and body weight. *Hum Mol Genet* **12**, 551–559.
- Xu J, Wang P, Li Y, Li G, Kaczmarek LK, Wu Y, Koni PA, Flavell RA & Desir GV (2004). The voltage-gated potassium channel Kv1.3 regulates peripheral insulin sensitivity. *Proc Natl Acad Sci U S A* **101**, 3112–3117.
- Xu L, Ki D, Zhu Y, Cai S, Liang X, Tang Y, Jin S & Ding C (2021). Swertiamarin supplementation prevents obesity-related chronic inflammation and insulin resistance in mice fed a high-fat diet. *Adipocyte* **10**, 160–173.
- Xu L, Kitade H, Ni Y & Ota T (2015). Roles of chemokines and chemokine receptors in obesity-associated insulin resistance and nonalcoholic fatty liver disease. *Biomolecules* **5**, 1563–1579.
- Yang Y, Smith DL, Keating KD, Allison DB & Nagy TR (2014). Variations in body weight, food intake and body composition after long-term high-fat diet feeding in C57BL/6J mice. *Obesity* **22**, 2147–2155.
- Yoshimura S, Nakashima S, Tomiga Y, Kawakami S, Uehara Y & Higaki Y (2018). Short- and long-term effects of high-fat diet feeding and voluntary exercise on hepatic lipid metabolism in mice. *Biochem Biophys Res Commun* **507**, 291–296.
- Zapiec B & Mombaerts P (2015). Multiplex assessment of the positions of odorant receptor-specific glomeruli in the mouse olfactory bulb by serial two-photon tomography. *Proc Natl Acad Sci U S A* **112**, E5873–E5882.
- Zhang C, Li D & Wang X (2020). Role of physical exercise type in olfactory deterioration in ageing. *Rhinology* **58**, 145–150.

Zheng C, Feinstein P, Bozza T, Rodriguez I & Mombaerts P (2000). Peripheral olfactory projections are differentially affected in mice deficient in a cyclic nucleotide-gated channel subunit. *Neuron* **26**, 81–91.

Additional information

Data availability statement

All data referenced in this report are summarized in the primary figures contained in the publication. All photomicrographs used to generate the summarized data are stored in the Fadool Laboratory and are available upon request.

Competing interests

The authors declare no financial or scientific conflicts of interest.

Author contributions

All authors critically evaluated the work for important intellectual content. All authors acquired, analysed, or interpreted data in the study. In using the CRediT (Contributor Roles Taxonomy) guidelines, B.C. and D.F. were responsible for project conceptualization, data curation, formal analysis, funding acquisition, methodology, validation, visualization, and writing the original draft, reviewing, and editing. B.C., A.L., D.G., D.L.C., C.H. and M.Q. were responsible for investigation and writing an original draft of the discussion. D.F. was responsible for project administration and supervision, and the provision of resources. All authors approved the final version of the manuscript; agreed to be accountable for all aspects of the work in ensuring that questions related to the accuracy or integrity of any part of the work are appropriately investigated

and resolved; and all persons designated as authors qualify for authorship, and all those who qualify for authorship are listed.

Funding

This work was supported by National Institutes of Health (NIH) grants R01DC013080, T32DC000044 and F31DC016817 from the National Institutes of Deafness and Communication Disorders (NIDCD); and an endowment from the Robinson Family and the Tallahassee Memorial Hospital.

Acknowledgements

We would like to thank Jessica Folsom, Henal Sutaria and Nimmi Patel for their technical assistance in maintaining running wheels, measuring body weights and collection of adipose tissues. We would like to thank Jaime White-James for the oversight of our animal husbandry and routine mouse care needs. We would like to thank Charles Badland, our departmental artist, for assistance with schematics. Cover art was designed by Charles Badland, Carley Huffstetler and Ashley Loeven; created with BioRender.

Keywords

diet, isocaloric, obesity, obesogenic, olfaction, pair feed

Supporting information

Additional supporting information can be found online in the Supporting Information section at the end of the HTML view of the article. Supporting information files available:

Peer Review History
Statistical Summary Document